GEAR TECHNOLOGY

The Journal of Gear Manufacturing

MAY/JUNE 1990

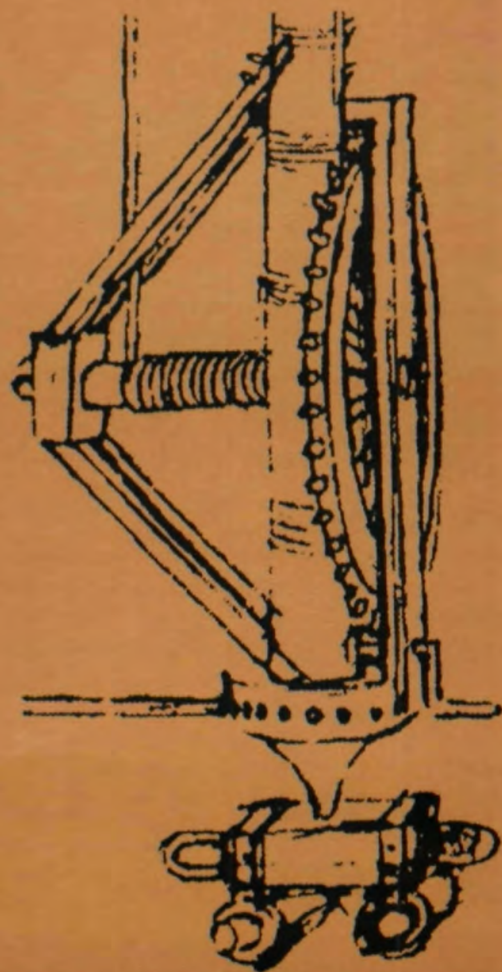

Comparative Load Capacity Evaluation of CBN-Finished Gears

Dynamic Loads in Parallel Shaft Transmissions — II

Geometric Design of Internal Gear Pairs

Shaper Cutters — Design & Application — II

GEAR TECHNOLOGY

PUBLISHER & EDITOR-IN-CHIEF
Michael Goldstein

ASSOCIATE PUBLISHER & MANAGING EDITOR
Peg Short

SENIOR EDITOR
Nancy Bartels

EDITORIAL ASSISTANTS
Laura Kinnane
Michelle Short

ART DIRECTOR
Jean Sykes

ADVERTISING SALES MANAGER
Patricia Flam

SALES COORDINATOR
Mary Michelson

CIRCULATION
Pamela Nolan
Debbie Donigian

RANDALL PUBLISHING STAFF: President, Michael Goldstein; Vice President, Richard Goldstein; Vice President/General Manager, Peg Short; Controller, Pat Nash; Accounting, Ruth J. Kussin; Art Consultant, Marsha Goldstein.

RANDALL PUBLISHING, INC.
1401 Lunt Avenue P.O. Box 1426
Elk Grove, IL 60007 (708) 437-6604

Our cover shows a detail view of a travelling crane as conceived by Leonardo da Vinci. It was designed to revolve on a pivot and lift heavy weights without being too cumbersome. It travelled on a small trolley with overhead guide wires and might have been used in the construction of tall buildings.

GEAR TECHNOLOGY

The Journal of Gear Manufacturing

CONTENTS

FEATURES

DEPARTMENTS

May/June, 1990 Vol. 7, No. 3

GEAR TECHNOLOGY, The Journal of Gear Manufacturing (ISSN 0743-6858) is published bimonthly by Randall Publishing Co., Inc., 1425 Lunt Avenue, P. O. Box 1426, Elk Grove Village, IL 60007. GEAR TECHNOLOGY, The Journal of Gear Manufacturing. Subscription rates are: $40.00 in the United States, $50.00 in Canada, $55.00 in all other foreign countries. Second-Class postage paid at Arlington Heights, IL and at additional mailing office.

Postmaster: Send address changes to GEAR TECHNOLOGY, The Journal of Gear Manufacturing, 1425 Lunt Avenue, P. O. Box 1426, Elk Grove Village, IL 60007.

MANUSCRIPTS: We are requesting technical papers with an educational emphasis for anyone having anything to do with the design, manufacture, testing or processing of gears. Subjects sought are solutions to specific problems, explanations of new: technology, techniques, designs, processes, and alternative manufacturing methods. These can range from the "How to . . ." of gear cutting (BACK TO BASICS) to the most advanced technology. All manuscripts submitted will be carefully considered. However, the Publisher assumes no responsibility for the safety or return of manuscripts. Manuscripts must be accompanied by a self-addressed, self-stamped envelope, and be sent to GEAR TECHNOLOGY, The Journal of Gear Manufacturing, P.O. Box 1426, Elk Grove, IL 60009, (708) 437-6604.

Before you buy a CNC Gear Inspection System, ask these four questions

1. Can we get complete inspection of both gears and cutting tools?

With the M & M 2000 QC System, the answer is yes. The system will test lead and involute profile characteristics of internal or external gears and splines. It is the only universal gear tester available which provides true index testing without expensive attachments. In addition, we have fully-developed software for checking hobs, shaver cutters, shaper cutters, and other cylindrical parts such as worms and cams.

Hob Pressure Angle Check

Shaver Cutter Lead Check

2. Can you customize software to meet our quality-inspection specifications?

At M & M Precision, we write and develop our own inspection software. Our technical team can and has implemented inspection specifications into specific software for individual requirements. Our current library includes line/curve fitting as well as modified K-chart analysis routines.

Line/Curve Fitting

Modified K-Chart Analysis

3. OK, you can inspect gears and cutting tools. What else is available to aid us in quality control of the manufacturing process?

At M & M Precision, we have fully integrated such advanced software packages as Statistical Process Control and Tooth Topography into our standard testing software. Our SPC program can identify non-random variations and provide early warning of variations which are approaching tolerance limits. Our Tooth Topography software features automatic testing of lead and involute at multiple locations and provides two- and three-dimensional graphics.

SPC Run Chart

Topological Map

4. Do you have the technical support team and installation experience to back up the hardware and software provided?

At M & M Precision, we have a technical team with over 45 man-years of experience in developing CNC gear inspection hardware and software. All software for our QC 2000 System has been developed in-house. In addition, we have working installations at these leading companies:

- General Motors
- TRW
- Ford Motor
- Warner Gear
- Cincinnati Milacron
- Chrysler
- Pratt & Whitney
- Rocketdyne

For details on our advanced QC 2000 System and available software, contact M & M Precision Systems, 300 Progress Road, West Carrollton, Ohio 45449, 513/859-8273.

M&M PRECISION SYSTEMS

AN ACME-CLEVELAND COMPANY

CIRCLE A-4 ON READER REPLY CARD

Editorial

LOOKING TO THE FUTURE

Six years ago this month, the very first issue of *GEAR TECHNOLOGY, the Journal of Gear Manufacturing,* went to press. The reason for starting the publication was a straightforward one: to provide a forum for the presentation of the best technical articles on gear-related subjects from around the world. We wanted to give our readers the information they needed to solve specific problems, understand new technologies, and to be informed about the latest applications in gear design and manufacturing. The premise behind *GEAR TECHNOLOGY* was also a straightforward one: the better informed our readers were about the technology, the more competitive they and their companies would be in the world gear market.

We've come a long way in the six years since the first issue when Randall Publishing had a two-desk office. Now our staff numbers ten, and we have an international reader and advertiser base. For this growth and success we have you, our subscribers and advertisers, to thank. Without your consistent support from the very beginning, *GEAR TECHNOLOGY* would not be the premier publication for gear manufacturing, design, and research.

Anniversaries are times to remember, consider accomplishments, evaluate goals, and, most important, plan for the future. We want to continue to merit your support. To do this, we need your help. We are constantly striving to bring you the best material available.

As our readership and our reputation have grown, we have started to receive more and more original manuscripts. *GEAR TECHNOLOGY* has become the publication of first choice for many of our authors. This means that our readers see more of the latest developments in gearing in our pages first. We will continue this trend in the future. But good contributors and good ideas are always a scarce commodity. If you have an article, a letter for our Viewpoint column, an idea for a new column, or some other way in which we could improve the content of *GEAR TECHNOLOGY,* please share it with us.

Keeping our mail list current is another challenge that you can help us meet. Letting our circulation department know about personnel changes, new mail stop numbers, and other "housekeeping" matters helps insure that copies of *GEAR TECHNOLOGY* get to where they are supposed to go. Filling out the information on this issue's wrap cover will help us spread the word about *GEAR TECHNOLOGY* to others who might be interested in it.

You may have noticed in the past few issues some changes in our type and design style. More of these will appear in the future. We want *GEAR TECHNOLOGY* to have an attractive, contemporary look and at the same time be as readable and "user friendly" as possible. We would like your feedback and comments on these changes as well. We pride ourselves on being, not only the most informative publication available about gearing, but also the best looking.

However, in spite of these cosmetic changes, our goals will remain the same — to bring you the best, most informative, up-to-date, technical information available about gear manufacturing, design, and research.

TECHNICAL CALENDAR

AGMA Technical Education Seminars, Series II. These one- or two-day seminars present the latest techniques and information on specific topics in a small group context. For more information contact AGMA, 1500 King St., Suite 201, Alexandria, VA 22314, (703) 684-0211.

MAY 8, 1990. Los Angeles, CA. **Controlling the Carburizing Process.** Presenting information on the selection of material, specifying case depth range, case microstructure, and minimum surface hardness.

JUNE 5-6, 1990. Alexandria, VA. **Gear System Design for Noise Control.** An overview of noise control in gear system design. Practical gear design is offered with a minimum of acoustical theory.

MAY 1-3, 1990. Houston Tool & Manufacturing Exposition, George R. Brown Convention Center, Houston, TX. For more information, contact: Houston Chapter, NTMA, 515 Post Oak Blvd., Suite 320, Houston, TX 77027. (713) 439-5890.

JUNE 7-10, 1990. AGMA Annual Meeting. The Homestead, Hot Springs, VA. This year's theme is "Gearing to Win." The program topics will be focused on competitiveness in the 90s and a review of the 332 Investigation.

SEPTEMBER 5-13, 1990. IMTS-90, McCormick Place, Chicago, IL. Largest trade show in the Western hemisphere with exhibitors from around the world. A new feature this year will be the 120,000 sq. ft. Forming and Fabricating Pavilion. For more information, contact: IMTS-90, 7901 Westpark Drive, McLean, VA 22102-4269. Ph:(703) 893-2900. Fax: (703) 898-1151.

OCTOBER 29-31, 1990. AGMA Fall Technical Meeting. Hilton International Hotel, Toronto, Canada. Papers and seminars on gear design, analysis, manufacturing, applications, gear drives, and related products. Contact AGMA Headquarters for further information.

Comparative Load Capacity Evaluation of CBN-Finished Gears

Raymond J. Drago, PE
Boeing Helicopters,
Philadelphia, PA

Abstract:

Cubic boron nitride (CBN) finishing of carburized gearing has been shown to have certain economic and geometric advantages and, as a result, it has been applied to a wide variety of precision gears in many different applications.

In critical applications such as aerospace drive systems, however, any new process must be carefully evaluated before it is used in a production application. Because of the advantages associated with this process, a test program was instituted to evaluate the load capacity of aerospace-quality gears finished by the CBN process as compared to geometrically identical gears finished by conventional grinding processes.

This article presents a brief description of the CBN process, its advantages in an aerospace application, and the results of an extensive test program conducted by Boeing Helicopters (BH) aimed at an evaluation of the effects of this process on the scoring, surface durability, and bending fatigue properties of spur gears.

In addition, the results of a x-ray diffraction study to determine the surface and subsurface residual stress distributions of both shot-peened and nonshot-peened CBN-ground gears as compared to similar conventionally ground gears are also presented.

Introduction

While CBN gear grinding is a relatively new technology, cubic boron nitride itself is not really a new material. It was developed more than 20 years ago by General Electric Company (under the trademark BORAZON) as a substitute for industrial diamonds. CBN is, as Fig. 1 indicates, quite hard and thus very resistant to wear. This high hardness relative to more conventional abrasives (such as aluminum oxide) used in grinding wheels, and the characteristic sharply angled shape of CBN crystals (Fig. 2)[1] combine to produce a grinding wheel that yields greatly improved performance in terms of both increased speed and consistent quality. These properties also contribute to the long life that is obtained from CBN wheels. Table I shows some of the applications of CBN; more detailed information related to the basic properties of CBN can be found in Reference 2.

Similarly, grinding with CBN is not new either; however, it is only in the last few years[3-5] that this technique has gained wide acceptance as a method for finishing precision gears. It can be applied to grinding a wide variety of gears, including spur, helical, bevel, and worms. In fact, any conventional gear-grinding process can be adapted to use CBN technology, although, as is discussed later, more than just the grinding wheel medium must change.

Our purpose here is neither to describe the basic process of CBN grinding nor to provide a comparison of the advantages and disadvantages of this process; however, a quick overview of both subjects will provide a better understanding of the reason this program was initiated and the real significance of the results.

The CBN Grinding Process

The CBN grinding process is actually more akin to a micromachining process than it is to our concept of conventional grinding. Material is removed by cutting away microscopically small chips, as opposed to the abrasion process that typifies conventional grinding.

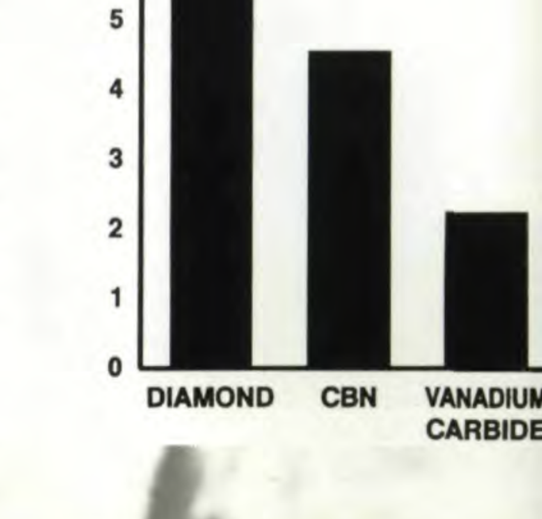

Both the actual grinding forces and the power required are higher for CBN than for conventional grinding. As a result, while most basic grinding processes can be readily adapted to the CBN process, the requirement for greater machine and work-holding stiffness indicates that, in most cases, existing machines cannot be used.

Many different types of CBN wheels are available. CBN wheels for gear-grinding purposes can generally be classified as either plated or bonded types. Plated types essentially have single CBN particles plated over the active wheel surface. Bonded wheels use a much thicker layer of CBN crystals, mixed with a variety of bonding agents, on the active surface of the wheel. Plated wheels cannot be dressed or trued but provide long life and consistent parts. Bonded wheels may (in fact, must) be dressed and thus provide the opportunity to vary tooth geometry, but with some sacrifice in part consistency.

Fig. 1—Hardness comparison of typical materials.

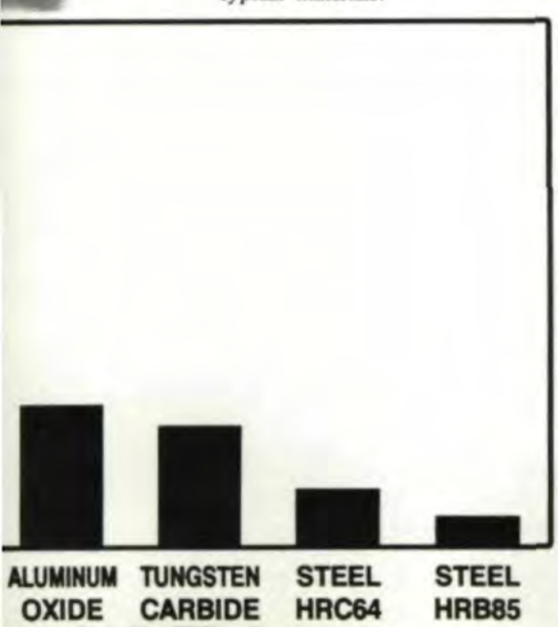

Table I. CBN Superabrasive Selection Chart

BORAZON CBN Type	Crystal Type	Mesh Size*	Wheel Bond	Recommended Applications
I	Monocrystalline; blocky shape, medium friability	40/60 to 325/400	Metal, vitreous, electro-plated	Steels hardened to Rockwell C50 and above; high-temperature superalloys with hardnesses of Rockwell C35 and above
II	Metal-coated Type I crystal	40/60 to 325/400	Resin	Same as Type I
500	Monocrystalline; blocky shape, tougher than Type I	60/80 to 325/400	Electro-plated	Same as Type I
510	Surface-treated Type 500 crystal	60/80 to 325/400	Metal, vitreous	Same as Type I; softer steels where abrasive pullout is a problem when grinding with Type I
550	Microcrystalline; irregular shape, high toughness, high thermal stability	20/30 to 140/170	Metal, vitreous	Hardened and soft ferrous alloys and cast irons
560	Metal-coated Type 550 crystal	20/30 to 140/170	Resin	Same as Type 550
570	Surface-treated Type 550 crystal	20/30 to 140/170	Electro-plated	Same as Type 550

* ASTME E-11 sleve. Types I and II CBN are also available as micron powders for fine grinding, lapping, and polishing. Data courtesy General Electric Company (from Reference 1)

Advantages

There are several reasons why CBN grinding technology is of interest to the gear designer, user, and manufacturer. Some are related to improved quality and consistency, while others are related to increased productivity and lower unit costs.

Reduced Burn Tendency. From the point of view of both manufacturing and design reliability, the fact that CBN technology promises to reduce the overall tendency to generate grinding burns is extremely attractive. Kumar[5] reports that, at room temperature, when grinding with a conventional aluminum oxide wheel, approximately 63% of the total heat generated goes into the work while only 37% goes into the wheel. By comparison, when grinding with a CBN wheel, about 96% of the total heat goes into the wheel while only 4% goes into the part. These observations are based on the thermal

Fig. 2 – Typical crystals of cubic boron nitride.

properties shown in Fig. 3. While this comparison is reasonable, it must be noted that actual values will vary substantially for any real grinding example, depending on the gear material and the actual wheel configuration. Still, the general trend is favorable since, with less heat delivered to the gear, the tendency to burn is markedly reduced.

This should not be interpreted, as some have, as indicating that it is not possible to burn parts when grinding with CBN. It is certainly possible to burn parts; it is just less likely that burning will occur. Things can go awry and the results can be disastrous with the best of processes.

Improved Wheel Life. One of the major problems associated with producing quality parts is the deterioration of the wheel with the number of linear inches of surface ground. As the life of the wheel improves, the consistency of the parts produced will also improve. The life of a typical CBN wheel is much longer, as Fig. 4 shows, than that for a conventional wheel. In reviewing this figure, it is important to note that two abscissa scales are used, and that the one for the CBN wheel is one hundred times that for the conventional wheel. It is clear, for this experiment at least, that the wear rate of the CBN wheel is 1/50 that of a conventional wheel.

Fatigue Life and Residual Stress. One of the benefits that have been claimed for CBN is a significant improvement in fatigue life and a related improvement in the residual stress profile for CBN parts. Figs. 5 and 6, which were abstracted from data obtained from Ref-

AUTHOR:

RAYMOND J. DRAGO *is a staff engineer with the Mechanical Dynamic Systems Technology Department of Boeing Helicopter. He is also chief engineer of Drive Systems Technology, Inc., a mechanical power transmission consulting organization. His areas of interest include applied mathematics, kinematics, analytical gear system design and synthesis, finite element analysis, and computer programming. Mr. Drago holds master degrees in engineering from the Pennsylvania State University and in structural engineering from Drexel University, and he is a licensed professional engineer in the State of Pennsylvania. He is a member of ASME and AGMA and is the author of numerous books and articles.*

erence 6 as presented in Reference 5, demonstrate improvements in both fatigue life and residual stresses for test specimens made from Rene 80. While we have no reason to doubt the veracity of these data, the testing was accomplished on a material that is not typically used for gears and by a grinding method that is not typical of gear tooth grinding techniques. The overall results are, however, intriguing and certainly worth further investigation.

It is this specific area that the program reported in this article was developed to evaluate. The basic question posed at the start of this program was "How do the bending, durability, and scoring load capacities of CBN parts compare to those of identical parts properly ground by conventional techniques with aluminum oxide wheels?" It was not our intent to prove a result; rather, our intent was to investigate a phenomenon and report the results.

The Program

In order to accurately compare the performance of typical aerospace-quality gears that were finished by conventional and CBN grinding techniques, a test program was defined. The gears used in this test program, for both the conventional and CBN grinding methods, were otherwise identical, within the limits normally allowed for aerospace gearing in general. That is, their basic geometry, accuracy, material, heat treatment, and all processing other than the tooth grinding were as nearly the same as practical for both configurations. These parameters are also representative of typical BH helicopter gears so that the data may be easily transferred to actual applications.

The specific test gear configurations and test rigs used were the standard BH rigs for each type of test and thus a large amount of historical data was available for comparative purposes.

Test Gear Configuration

Two types of gears were tested as shown in Table II. Both are fully representative of typical helicopter gears except for face width. The differences in configuration are necessary to accommodate differences in the test rigs used for each test.

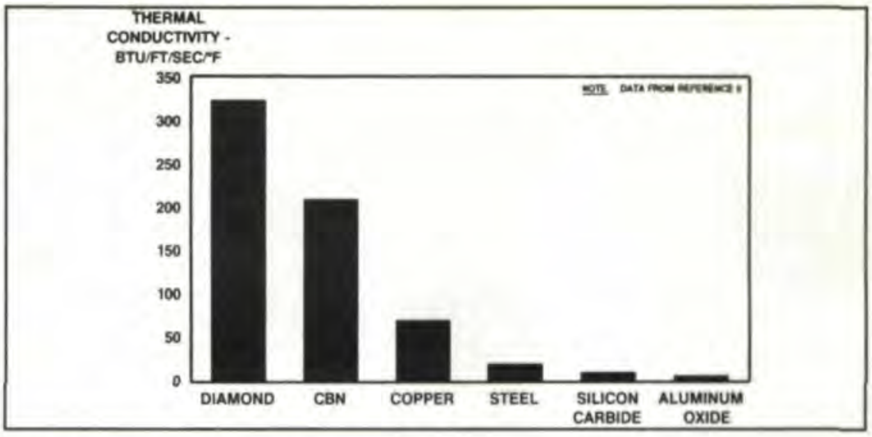

Fig. 3 – Comparison of thermal conductivity at room temperature.

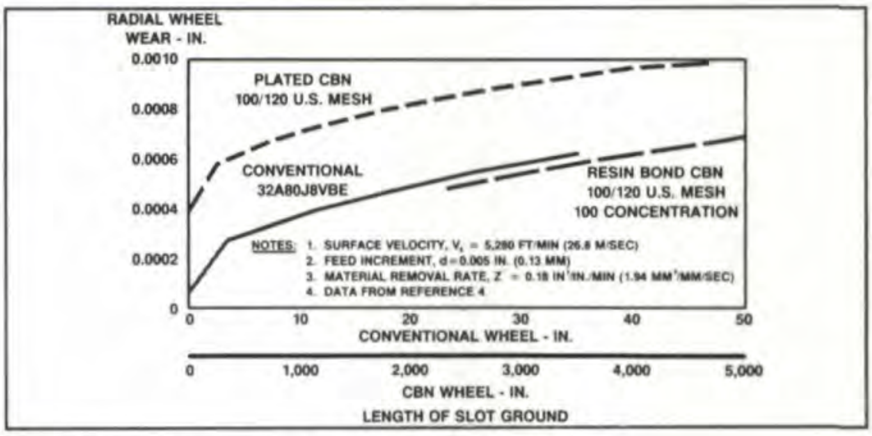

Fig. 4 – Laboratory comparison of wear rate of grinding wheels.

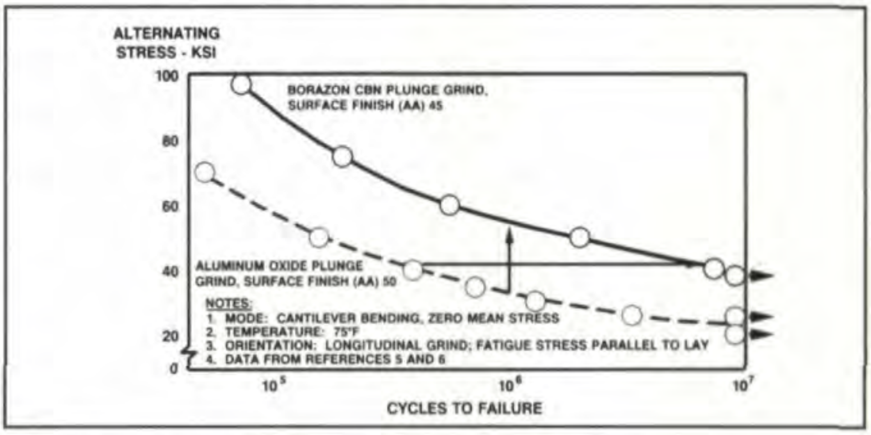

Fig. 5 – Fatigue characteristics of Rene 80 produced by plunge grinding.

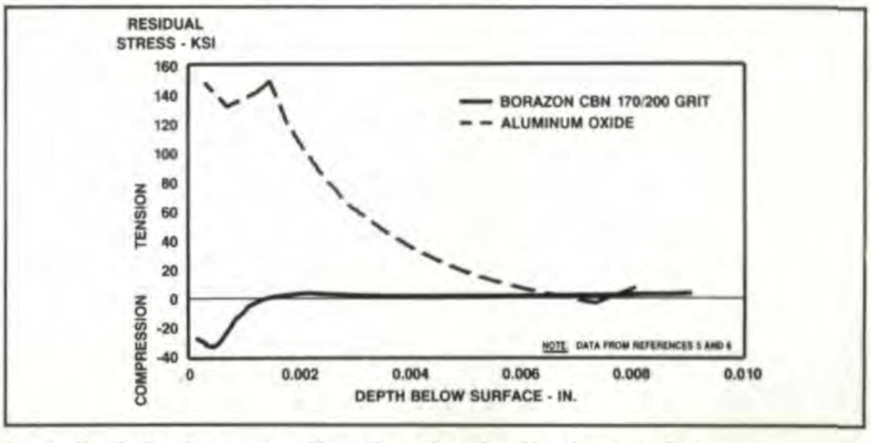

Fig. 6 – Residual surface stress profiles in Rene 80 produced by plunge grinding.

Table II. Test Gear Configurations

Parameter	Bending Fatigue	Scoring and Durability
Type	Spur	Spur
Diametral Pitch (in.)	5.3333	5.0
Pressure Angle (deg)	25.	25.
Number of Teeth	32.	30.
Quality Level, Q_n	12 - 13	12 - 13
Material	AISI 9310 DVM (BMS 7-249, Type III)	AISI 9310 DVM (BMS 7-249, Type III)
Surface Hardness	HRC 60-64	HRC 60-64
Effective Case Depth (at HRC 50) (in.)	0.035-0.055	0.030-0.045
Core Hardness	HRC 32-42	HRC 32-42
Surface Finish (max)	25 RMS	25 RMS

All gears were form-ground with full circular fillets. All CBN test specimens were shot-peened per our normal production specification. The advantage of using these specific configurations for the test parts is that they represent standardized test components that have been used for over 20 years in similar test programs; thus, the reliability of the specimens and their application to the final product are well-documented and understood. In addition, a large and varied test data history is available for comparative purposes. The small differences in pitch and case depth simply accommodate differences in the test rigs used for the bending and surface loads tests.

Test Gear Manufacture

The test gears were manufactured in accordance with normal Boeing Helicopter's standards by a qualified supplier. The results of all inspections conducted on the as-manufactured parts indicated that they were within typical expected ranges for other parts of similar size and configuration and were representative of the results for geometrically identical test gears from previous programs.

The only significant difference noted between the CBN-ground gears and previous test gears is that the surface finish on the CBN test gears hovered near the limit, typically 20-25 RMS, while most previous conventionally ground gears were found to be well below the limit on surface finish, typically 14-18 RMS.

The surface finish on the CBN parts could be improved by using a finer grade wheel (i.e., smaller CBN particles). If this is done with a plated wheel, however, wheel life may suffer somewhat. Use of a finer wheel of the bonded type will improve finish, but will sacrifice some part-to-part consistency.

Single-Tooth Bending Fatigue Testing

In order to evaluate the relative bending fatigue capacity of CBN and conventional gears, a series of carefully controlled single-tooth bending fatigue tests were run.

Test Fixture. The fixture used (Fig. 7) is the standard BH single tooth rig. It applies a unidirectional load to one tooth at a time. A total of four teeth per specimen are typically tested, although this can be increased to eight with a special adapter. The fixture is installed in a universal fatigue test machine (in this case, a Baldwin-Lima-Hamilton IV-20) capable of applying 16,000 pounds of total test load (8,000 pounds steady, plus 8,000 pounds alternating) at a frequency of 1,200 cycles per minute. The fixture is designed so that the load is applied to the test tooth at the highest point of single-tooth contact (based on a 1:1 ratio), while the reaction anvil contacts the reaction tooth at the lowest point of single-tooth contact. A constant load of 100 pounds is maintained on the test tooth at all times to prevent the impact loading that would occur if the load went through zero.

Instrumentation. The only instrumentation required for this test was that necessary to monitor test time (cycles of load application) and a crackwire signal. The crackwire provided automatic machine shutdown and test termination when the crack reached a specific, predetermined length, so that all failures were uniform. The crackwire was positioned on all gears so that a crack of approximately 0.070 - 0.080 inch would break the wire and cause an automatic shutdown.

A high-amplitude microswitch was also provided as a backup. This switch sensed abnormal movements of the machine that might occur in the event of an unexpected failure of the machine or the test specimen and automatically shut down the machine.

Calibration. Before the start of the test, the load link and one of the test gears were instrumented with strain gages. The test gear was gaged as shown in Fig. 8 so that actual gear tooth root stresses could be measured. The location of the strain gages on the test gears was determined by calculation of the critical section based on the standard AGMA approach and by examination of the failure origins from previous test gears. Since these test gears are quite thick-rimmed, the measured stresses should match those predicted by the AGMA method relatively closely. As Fig. 9 shows, there was good correlation.

Procedure. The testing procedure was quite simple. The test gear was installed in the fixture, and the height of the load anvil was adjusted to the required position (highest point of single-tooth contact) as determined by gear and fixture geometry. The load anvil was then checked for proper positioning. A steady load of 100 pounds was applied to the test tooth, and all dimensions were rechecked. The steady load was maintained approximately 100 pounds above the alternating load at all test conditions to prevent impact loading of the teeth.

Once the gear position was checked, the desired load was applied and the machine turned on. A small amount of moly grease was used at the tooth/anvil contact points to prevent fretting. During the course of the testing the specimen was checked for localized heating. At no time did the specimen

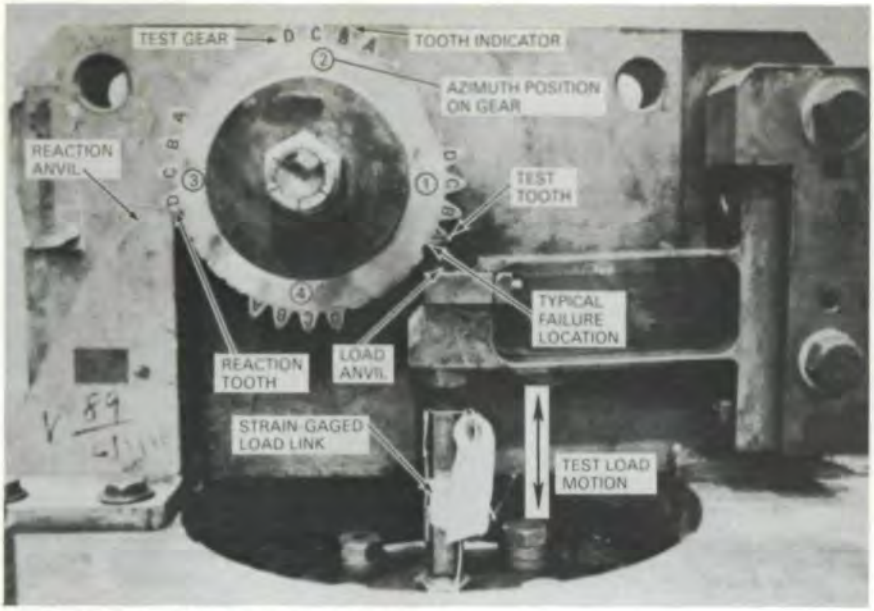

Fig. 7 – Single-tooth bending fatigue test fixture.

temperature exceed the ambient room temperature by more than 20°F. Each specimen was run at the specified load unit failure or 10 million cycles, whichever occurred first. Runouts were determined by cycle count. Failure was defined as a crack that progressed sufficiently to break the crackwire, at which point the machine was shut down automatically. This procedure insured that all failures were uniform.

Results. A total of twelve data points, eleven failures, and one runout, were obtained. The data were analyzed in accordance with standard BH statistical methods.[7] The results of this analysis are presented in Fig. 10. In order to provide a basis for comparison, similar data for two previous test programs, using identical gears, but convention-

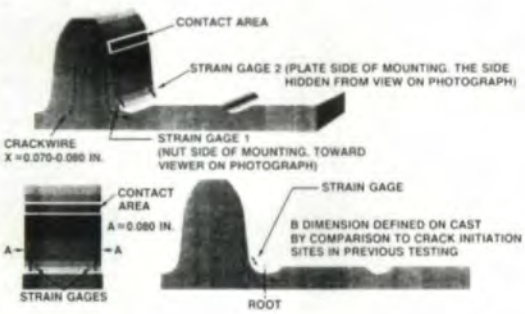

Fig. 8 – Strain gage and crackwire placement.

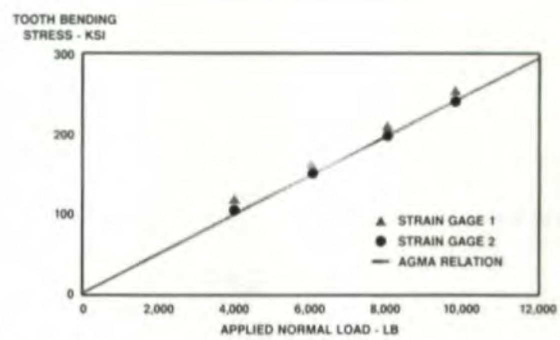

Fig. 9 – Single-tooth bending calibration and correlation.

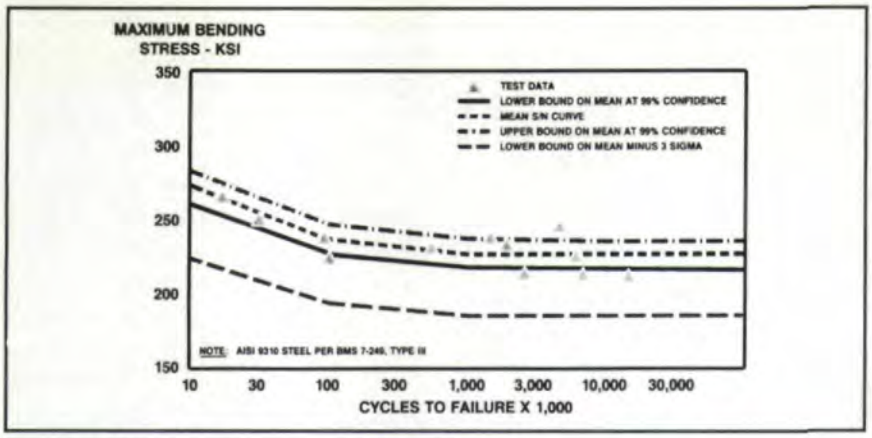

Fig. 10 – Single-tooth bending fatigue data for CBN-ground gear.

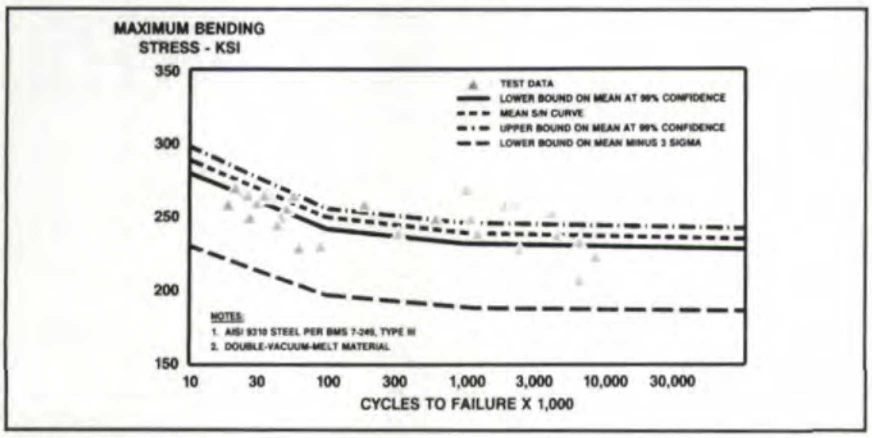

Fig. 11 – Single-tooth bending fatigue data for conventionally ground gear of vacuum-carburized steel.

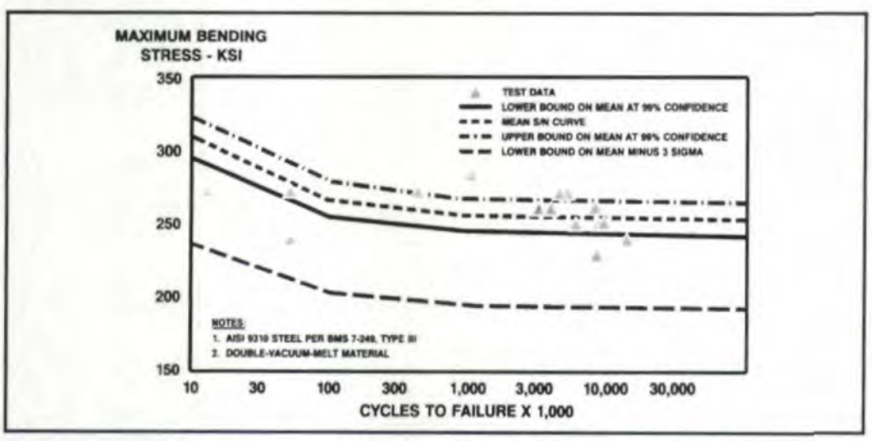

Fig. 12 – Single-tooth bending fatigue data for conventionally ground gear of gas-carburized steel.

Fig. 13 – Rig for rotating surface durability and scoring test.

Fig. 14 – Gear research test facility.

ally ground with aluminum oxide wheels, are shown in Figs. 11 and 12. While the mean endurance limits for these three tests vary somewhat, the mean-minus-three-sigma (standard deviation) limits are remarkably similar. Much information that is not at first obvious is conveyed by these three charts.

Durability and Scoring Testing

Test Rig. The test rig used for both the durability and scoring test phases of this program is shown in Figs. 13 and 14. This four-square, locked-in-torque rig is capable of testing spur or helical gears on 6-, 10-, or 16-inch center distances. Two test configurations at each center distance, overhung and straddle-mounted, are possible with this rig. When mounted in the overhung configuration, as shown in Fig. 13, the gears are wholly contained within a housing that is external to all other rotating components. This allows the test gear lubrication system to be fine-tuned exactly to the configuration being tested. The test oil thus lubricates nothing but the test gears, so cross-contamination is avoided. Precise control of flow, pressure, and temperature, as well as oil jet impingement on the test gears themselves, is carefully maintained.

The stand is capable of testing up to a pitch-line velocity of 10,000 feet per minute at more than 50,000 in.-lb of pinion torque. All gears and bearings, both test and slave, are pressure-jet lubricated with MIL-L-23699 oil. Power is supplied by a 100-hp motor running at 3,600 rpm. Variations in shaft speed are provided by changing the timing pulley configuration between the motor and the test stand input shaft.

Each gearbox on the rig (two slave and one test) is lubricated with a separate, completely self-contained oil system. Each system consists of both pressure and scavenge pumps with in-line heat exchangers, pressure and temperature sensors, and a very-high-capacity fine filtration system (3, 12, 25 micron; 12 used for this testing). The test gearbox is also equipped with an in-line, high-capacity heater that allows the actual oil inlet temperature at the test gear jet to be controlled within 5°F.

Instrumentation. The major variable in both the scoring and durability testing is shaft torque; thus, shaft torque measurement is provided. In addition, the stand is instrumented to provide information on oil flow rate, pressure, temperature (into and out of the test unit), and run time. Vibration measurement is also available, but was not used in this testing.

Calibration. Before the start of the test program, the instrumented shaft that is used to measure torque is calibrated (actually calibrated twice since a redundant torque bridge is provided for reliability). The oil flow and temperature sensors to the test gear set are also calibrated and certified.

In addition, all gearboxes are drained, flushed, and refilled with the test lubricant to insure that the oil systems are free of any possible contaminants from previous testing.

Procedure. At the start of the test, all oil lubrication pumps were started and run until a stable temperature condition was observed. At that point, the desired torque was applied to the pinion shaft within an accuracy of 5%.

The specific test conditions for the scoring and durability tests were slightly different as Tables III and IV show.

The durability tests were run for 7 million cycles or until failure, whichever occurred first. Failure was determined by the occurrence of a minimum of one pit, at least 1/16 by 1/16 inch in size, on at least three nonadjacent teeth. A gear that completed 7 million cycles was considered a runout.

The scoring tests were run according to the procedure outlined in Fig. 15. Testing continued by this procedure until failure; thus the scoring testing produced no runout points.

Durability Results. A total of ten data points, eight failures, and two runouts, were obtained. As was the case with the bending data, these data were analyzed in accordance with standard BH statistical methods.[7] The results of this analysis are presented in Fig. 16. In order to provide a basis for comparison, similar data for a previous test program, using identical gears, but conventionally ground with aluminum oxide wheels, are shown in Fig. 17. While the mean endurance limits for these two tests vary considerably, the mean-minus-three-sigma (standard deviation) limits almost overlie one another.

Scoring Results. A total of ten scoring data points were obtained from this

Table III. Durability Test Conditions

Pinion Speed	3,600 rpm
Oil Inlet Temperature	135°F
Oil Jet Pressure	45 psi
Oil Jet Flow	0.32 gpm

Table IV. Scoring Test Conditions

Pinion Speed	3,600 rpm
Oil Inlet Temperature	200°F
Oil Jet Pressure	45 psi
Oil Jet Flow	0.32 gpm

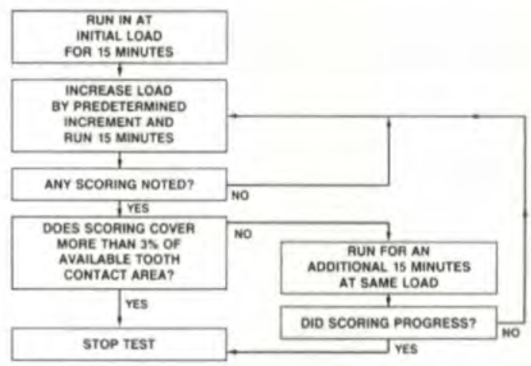

Fig. 15 – Scoring test procedure.

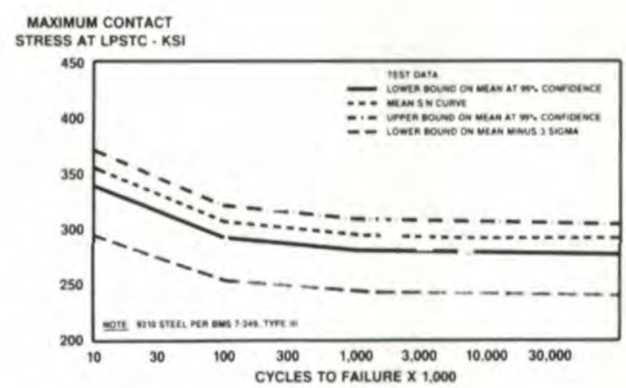

Fig. 16 – Tooth surface durability data for CBN-ground gear.

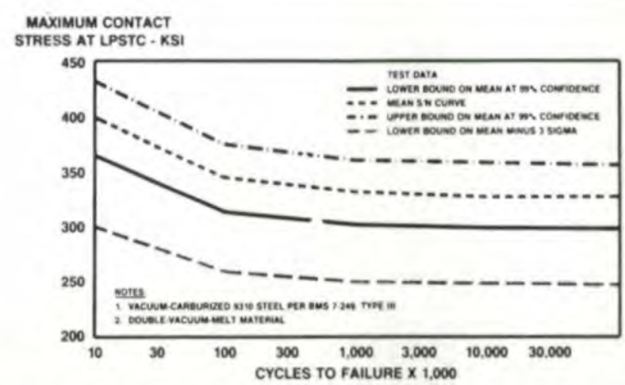

Fig. 17 – Tooth surface durability data for conventionally ground gear.

testing. The results were analyzed statistically based on a normal distribution so that the scoring probability curve shown in Fig. 18 could be developed. For reference purposes, the curve obtained from a similar test program with conventionally ground spur gears is superimposed on the same figure. The difference between the two curves is insignificantly small.

The additional line shown in Fig. 18 denote AISI 9310 gears that were carburized, hardened, and conventionally ground. The data for these other oils, presented for comparative reference only, were obtained either from similar R&D testing or by ratioing Ryder-type data to fit the format shown. The data shown are valid for reference purposes, but their use in design must be modified by appropriate safety factors to account for increased data uncertainty relative to the MIL-SPEC oils.

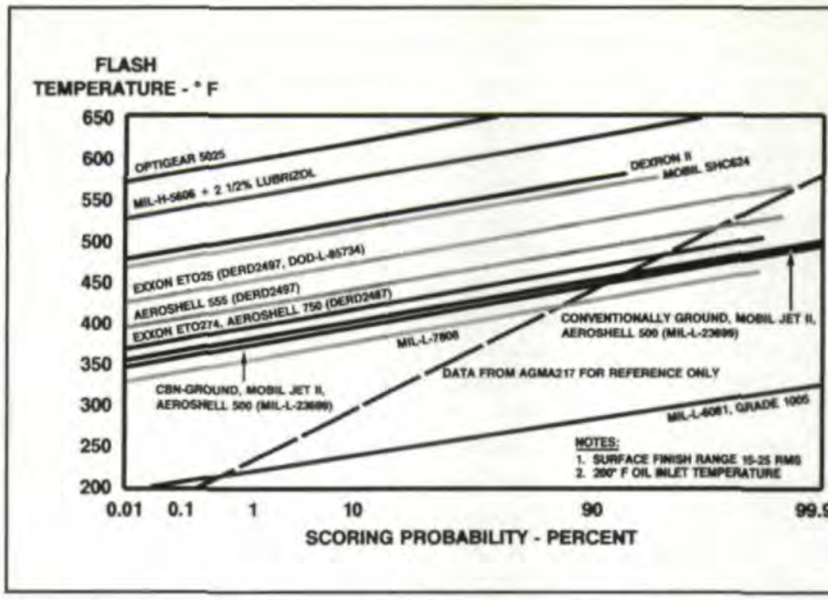

Fig. 18 – Scoring probability of conventionally and CBN-ground spur test gears.

Discussion

Based on the data presented here, it appears that there is not a significant difference in the load capacity of gears that have been finished by CBN grinding when compared to exactly identical gears that have been finished by conventional methods with aluminum oxide wheels. This observation would seem to contradict the data shown in Fig. 5 in which the CBN process is credited with a substantial improvement in the bending fatigue capability of parts that were CBN-ground when compared to conventionally ground parts. However, several factors must be considered before proceeding further.

First and foremost, the data presented in Fig. 5 are neither based on gear tooth testing nor is the material one that would be used for a gear. In addition, all of the gears that were used in the testing reported herein were shot-peened all over after final grind.

The major difference, however, may well be that these gears are all (both conventional and CBN) of typical helicopter main power train quality. This being the case, both the conventional and the CBN grinding processes are very carefully controlled and monitored so that problems related to burning and other heat-related distress do not occur in the finished parts.

If the conventional grinding process is carefully controlled, it will produce parts that are free of even minimal distress. Conversely, if it is not carefully controlled and monitored, parts with high residual tensile stresses and possibly some burns can become part of a given lot of parts, thus reducing the overall average load capacity. Since one of the main advantages of the CBN process is its relative insensitively to such problems, it stands to reason that, when compared to conventional grinding of commercial quality, it is possible that the CBN parts may show an improvement in fatigue life. This improvement is, however, plainly not evident when CBN parts are compared with very high-quality parts made by conventional techniques.

This is not to say that the use of CBN grinding is of no advantage. This testing simply indicates that, for helicopter-quality gears, no load capacity advantage is obtained through the use of CBN gears.

Considerable advantage can be obtained, even for helicopter-quality gears, through use of CBN gears due to improvements in productivity and consistency of parts. In fact, based on the favorable results of this program, CBN grinding has been approved as a production process for several current applications with good results.

Residual Stresses

One of the advantages that is frequently claimed for CBN parts[4-5] is the existence of a residual compressive layer on the ground tooth surfaces after CBN finishing. The implication is, of course, that the residual stress profile produced by conventional grinding is poor by comparison.

As noted above, based on the favorable results of this program, the CBN process was ultimately approved for use on 9310 steel production gears. Before this approval was granted, however, completed destructive metallurgical evaluations were performed on several of these production parts. Specifically, comparative evaluations were conducted on conventionally ground production parts and on the proposed CBN-ground replacement parts. In general, the two types of finishing methods produced parts of like metallurgical characteristics. As part of the metallurgical evaluation, residual stress measurements were taken by x-ray diffraction techniques on both types of parts before and after shot-peening. The results of these measurements are shown in Figs. 19 and 20 for the CBN and conventionally ground parts, respectively. These production parts are 10 diametral-pitch, 19,000-rpm helical gears transmitting about 2,000 horsepower.

While the CBN-ground gears do exhibit a very shallow compressive stress layer, the properly conventionally ground gears also show a similar shallow compressive stress layer. This compressive layer is, however, much enhanced by proper shot-peening on both the CBN and conventionally ground gears, as is evident from these plots.

(continued on page 48)

Dynamic Loads in Parallel Shaft Transmissions — Part 2

Hsiang-Hsi (Edward) Lin, Memphis State University, Memphis, TN;
Ronald L. Huston, University of Cincinnati, Cincinnati, OH;
John J. Coy, NASA Lewis Research Center, Cleveland, OH

AUTHORS:

DR. HSIANG HSI LIN *is on the faculty at Memphis State University. His research includes kinematics, dynamics, optimization, finite element methods, and computer-aided design and analysis of mechanical systems. He received his undergraduate degree from National Chung Hsing University and did his graduate work at the University of Cincinnati.*

DR. RONALD L. HUSTON *is Professor of Mechanics at the University of Cincinnati and Director of the University's Institute for Applied Interdisciplinary Research. He earned his degrees in Mechanical Engineering and Engineering Mechanics from the University of Pennsylvania.*

DR. JOHN J. COY *is Branch Chief, Rotorcraft Systems Technology in the Propulsion Systems Division at NASA Lewis Research Center in Cleveland, OH. He took his degrees in Mechanical Engineering from the University of Cincinnati. He is the author of numerous papers and is a member of ASME. Dr. Coy is a licensed professional engineer in the State of Ohio.*

Summary:

Solutions to the governing equations of a spur gear transmission model, developed in a previous article are presented. Factors affecting the dynamic load are identified. It is found that the dynamic load increases with operating speed up to a system natural frequency. At operating speeds beyond the natural frequency the dynamic load decreases dramatically. Also, it is found that the transmitted load and shaft inertia have little effect upon the total dynamic load. Damping and friction decrease the dynamic load. Finally, tooth stiffness has a significant effect upon dynamic loading: the higher the stiffness, the lower the dynamic loading. Also, the higher the stiffness, the higher the rotating speed required for peak dynamic response.

Introduction

The development of a simple parallel shaft spur gear transmission model with its dynamic differential equations and solution procedures were presented in Reference 1. Various parameters such as inertia, stiffness, friction, and damping were included in the governing equations for further study.[1]

The purpose of this report is to determine the effect of these parameters on gear dynamic load. The dynamic load of a gear transmission can be found by solving the governing equation. The solution is known as the dynamic motion of the gear transmission. This dynamic motion can then be substituted into other analytical formulae and solved for gear dynamic loads.

A model of the transmission is depicted in Fig. 1. The governing equations are:

$$J_M\ddot{\theta}_M + C_{s1}(\dot{\theta}_M - \dot{\theta}_1) + K_{s1}(\theta_M - \theta_1) = T_M \quad (1)$$

$$J_1\ddot{\theta}_1 + C_{s1}(\dot{\theta}_1 - \dot{\theta}_M) + K_{s1}(\theta_1 - \theta_M) + C_g(t)[R_{b1}\dot{\theta} - R_{b2}\dot{\theta}_2] + K_g(t)[R_{b1}(R_{b1}\theta_1 - R_{b2}\theta_2)] = T_{f1}(t) \quad (2)$$

$$J_2\ddot{\theta}_2 + C_{s2}(\dot{\theta}_2 - \dot{\theta}_1) + K_{s2}(\theta_2 - \theta_1) + C_g(t)[R_{b2}\dot{\theta}_2 - R_{b1}\dot{\theta}_1] + K_g(t)[R_{b2}(R_{b2}\theta_2 - R_{b1}\theta_1)] = T_{f2}(t) \quad (3)$$

$$J_L\ddot{\theta}_L + C_{s2}(\dot{\theta}_L - \dot{\theta}_2) + K_{s2}(\theta_L - \theta_2) = -T_L \quad (4)$$

where J_M, J_1, J_2, and J_L represent the mass moments of inertia of the motor, the gears, and the load; C_{s1}, C_{s2}, and $C_g(t)$ are damping coefficients of the shafts and the gears; K_{s1}, K_{s2}, and $K_g(t)$ are stiffness of the shafts and the gears; T_M, T_L, $T_{f1}(t)$, and $T_{f2}(t)$ are motor and load torques and frictional torques on the gears; R_{b1} and R_{b2} are base circle radii of the gears; t is time; and the overdots indicate time differentiation.

In this report we present the results of numerical solutions of Equations 1 to 4 for a typical transmission system. A flow chart outlining the numerical procedure is presented. Natural frequencies are determined. The dynamic load is determined. Finally, the dynamic factor defined as the ratio of the dynamic load to the static load, is determined.* The results are calculated as functions of the rotating speed and roll angle for a variety of damping and stiffness conditions.

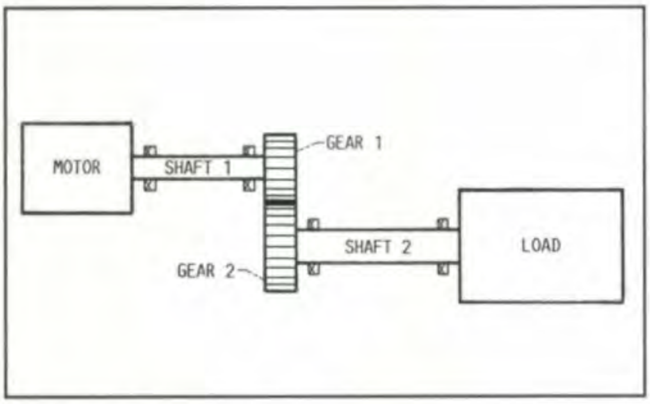

Fig. 1 – A simple spur gear system.

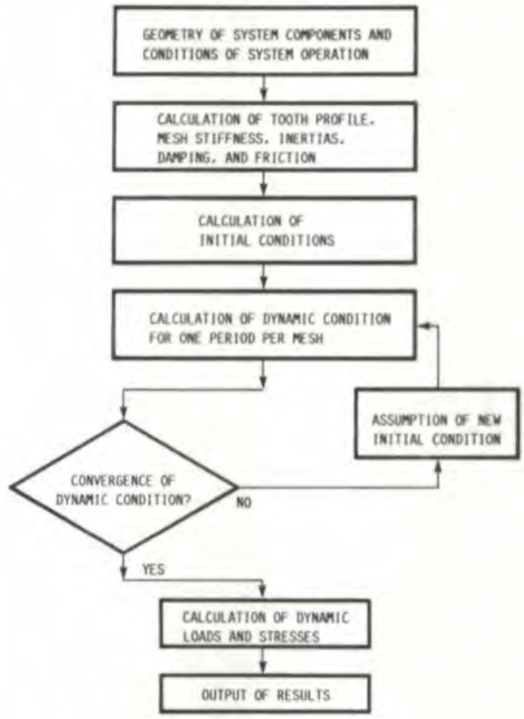

Fig. 2 – Flow chart of computational procedure.

Procedure

Fig. 2 presents a flow chart of the computational procedure used in the parameter study. The procedure is the same as that outlined at the end of Reference 1.

In conducting the analysis it is useful to compare the locations of the peak dynamic loads with the locations of the system natural frequencies (or critical speeds). The natural frequencies themselves may be obtained by examining the undamped equations of motion. These equations may be written in the matrix form:

$$[J]\,[\ddot{\theta}] + [K]\,[\theta] = [0] \qquad (5)$$

where the inertia matrix [J] is

$$[J] = \begin{bmatrix} J_M & O & O & O \\ O & J_1 & O & O \\ O & O & J_2 & O \\ O & O & O & J_L \end{bmatrix} \qquad (6)$$

*The term "dynamic factor" or "dynamic load factor" has been used inconsistently in the literature. The American Gear Manufacturer's Association (AGMA) dynamic factor, K_v, is used as a strength reduction factor and is defined as the maximum static load divided by the maximum dynamic load. This paper will follow the ISO convention, which uses the dynamic factor, K_d, as a load/stress increasing factor. Therefore, $K_d = 1/K_v$.

NOMENCLATURE

- C_g damping coefficient of gear tooth mesh, N-sec (lb-sec)
- C_s damping coefficient of shaft, N-m-sec (in.-lb-sec)
- J_L polar moment of inertia of load, kg-m^2 (in.-lb-sec^2)
- J_M polar moment of inertia of motor, kg-m^2 (in.-lb-sec^2)
- J_1 polar moment of inertia of gear 1, kg-m^2 (in.-lb-sec^2)
- J_2 polar moment of inertia of gear 2, kg-m^2 (in.-lb-sec^2)
- K_d dynamic factor
- K_g stiffness of gear tooth, N/m-rad (in./lb-rad)
- K_s stiffness of shaft, N-m/rad (in.-lb/rad)
- K_v AGMA dynamic factor, $Kv = 1/K_d$
- R_b base radius, m (in.)
- R_p pitch radius, m (in.)
- T_L torque on load, N-m (in.-lb)
- T_M torque on motor, N-m (in.-lb)
- T_{f1} torque on gear 1, N-m (in.-lb)
- T_{f2} torque on gear 2, N-m (in.-lb)
- W applied load, N (lb)
- θ angular displacement, rad
- $\dot{\theta}$ angular velocity, rad/sec
- $\ddot{\theta}$ angular acceleration, rad/sec^2
- ω_n natural frequency, Hz
- ξ damping ratio

and the stiffness matrix [K] is

$$[K] = \begin{bmatrix} K_{s1} & -K_{s1} & 0 & 0 \\ -K_{s1} & K_{s1} + (K_g)_{avg}R^2_{b1} & -(K_g)_{avg}R_{b1}R_{b2} & 0 \\ 0 & -(K_g)_{avg}R_{b1}R_{b2} & K_{s2} + (K_g)_{avg}R^2_{b2} & -K_{s2} \\ 0 & 0 & -K_{s2} & K_{s2} \end{bmatrix} \quad (7)$$

where $(K_g)_{avg}$ represents the average value of the gear mesh stiffness. It is taken as the sum of the discrete tooth stiffness values of a mesh cycle divided by the number of mesh positions in the cycle.

In the parameter study the system had identical gears with the following properties:

Number of teeth 36
Module, mm . . . . 3.18 (8 diametral pitch)
Pitch diameter, m (in.) 0.1143 (4.5)
Pressure angle, deg 20
Applied load, N (lb) 2670 (600)
Face width, m (in.) 0.0254 (1.0)
Moment of inertia,
  kg m^2 (in.-lb-sec^2) . . 3.3323×10^{-3} (0.02947)
Average tooth stiffness, N m/rad
  (lb-in./rad) . . . . . . 3.991×10^5 (3.5355×10^6)
Damping ratio 0.10
The shaft stiffness and inertias were:
Shaft stiffness, N m/rad
  (in.-lb/rad) 1138.17 (10081)
Load inertia and motor inertia, kg m^2
  (in.-lb-sec^2) . . . . 9.989×10^{-3} (each) (0.08841)

Results

Using the aforementioned data in the gear system model shown in Fig. 1, the natural frequencies of the four degrees of freedom model were found to be

$$\begin{array}{ll} \omega_{n1} = 0 \text{ (rigid body mode)} & \omega_{n2} = 1.49 \text{ Hz} \\ \omega_{n3} = 2.99 \text{ Hz} & \omega_{n4} = 144.8 \text{ Hz} \end{array} \quad (8)$$

The first three natural frequencies are well below tooth meshing frequencies and are, therefore, not of interest in this analysis (although they can still be excited by shaft eccentricity, which is not modeled here). The fourth natural frequency matches tooth meshing frequency at the critical speed of 8688 rpm, which is within the operating range of the gears.

Fig. 3 shows the variation of dynamic load response for a pair of teeth as a function of roll angle. At speeds much lower than the critical speed, the dynamic load response is basically a static load sharing in phase with the stiffness change, superimposed with an oscillatory load at a frequency corresponding to the natural frequency.

At higher speed, close to the critical speed, the dynamic load variation becomes so abrupt that it produces tooth separation. The peak dynamic load is much higher than the static load and is very likely to be a source of gear noise and early surface fatigue.

Fig. 4 shows the dynamic factor K_d as a function of operating speed. Prominent peaks (resonances) may be seen at speeds of 7650 and 4200 rpm. The larger peak 7650 rpm occurs at 88% of the calculated critical speed. The experimental work by Kubo[6] reported a similar result: that the critical speed was found at about 90% of the calculated critical speed. The second peak at 4200 rpm is a nonlinear effect of the time varying tooth stiffness known as the parametric resonance. This parametric resonance frequency occurs at about one-half

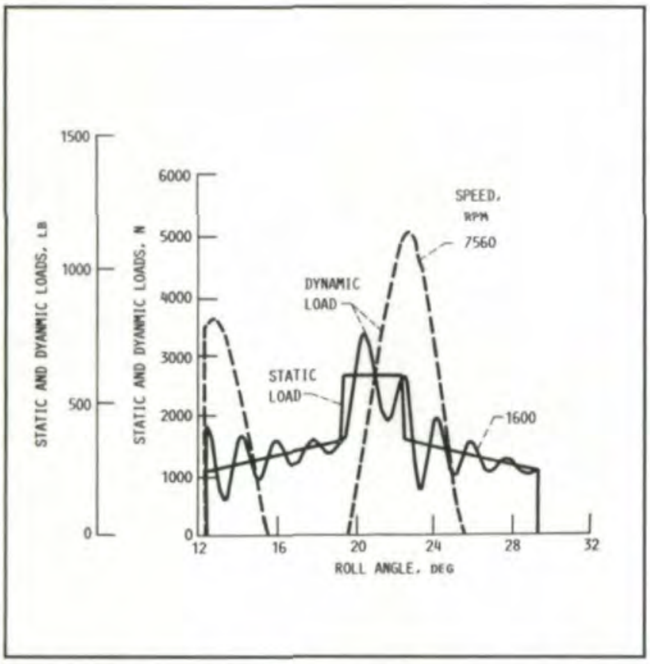

Fig. 3 – Dynamic loads at different speeds for identical years. Module = 3.18 mm; pressure angle = 20°; pitch radii = 57.1 mm; applied load = 2760 N (600 lb.).

of the critical speed.[2] For speeds above the critical speed, the dynamic response decreases steadily in the same manner as with elementary vibrating systems.

Fig. 5 shows a three-dimensional representation of the system dynamic response. The horizontal axis represents the operating speed, and the contact position along the tooth profile. The total number of contact positions is 121. The vertical axis is the dynamic factor.

Fig. 6 presents a contour plot of the system dynamic response. The shaded areas represent regions where tooth separation occurs. They are located in the double contact regions. At near resonance speeds the vibration amplitude exceeds the deflection of the meshing teeth, thus inducing tooth separation.

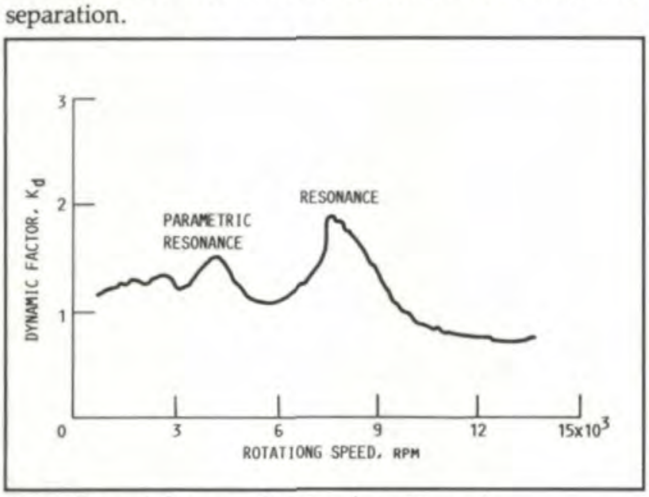

Fig. 4 – Dynamic factor as a function of rotating speed.

As the speed increases, the dynamic response also shows a phase shift toward the higher numbered contact positions. This phenomenon can be seen by noting that at speeds from 600 to 4200 rpm (one-half subharmonic), the maximum dynamic load occurs at double- to single-contact transitions (position 51) and gradually changes to single- to double-contact transitions (position 75). At speeds between one-half subharmonic and resonance, the maximum peak stays near the single- to double-contact transitions. After the speed

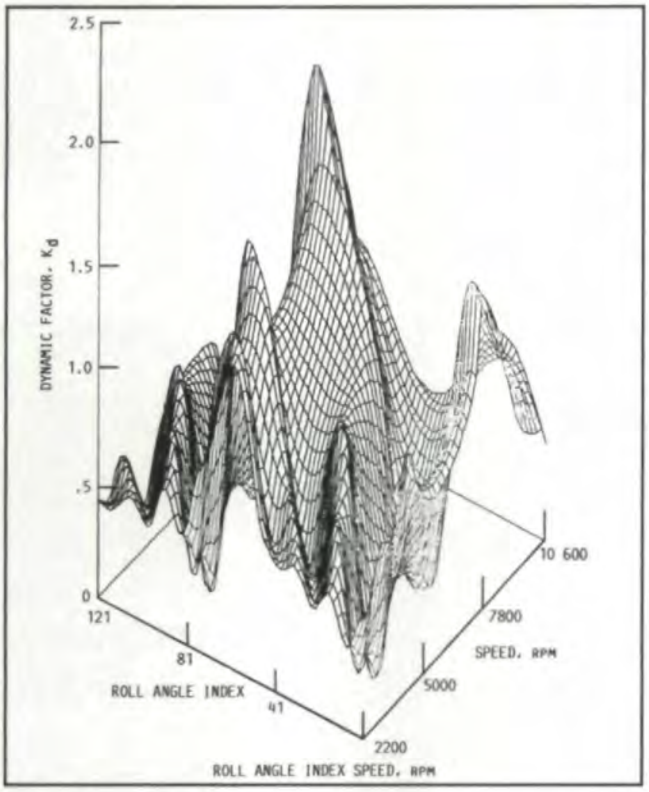

Fig. 5 – System dynamic response.

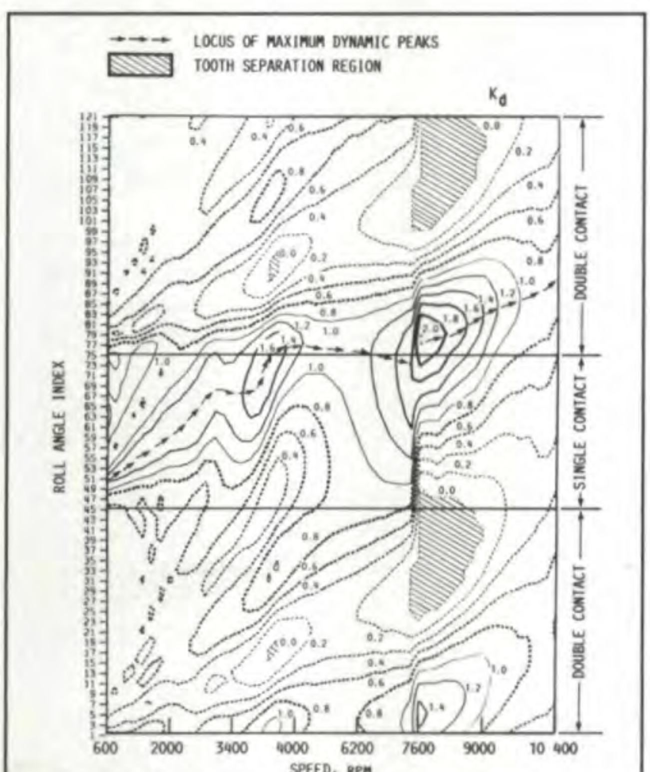

Fig. 6 – Contour plot of system dynamic response.

passes resonance, the major dynamic peak moves again towards higher contact positions on tooth profile with increasing speed.

Fig. 7 shows the dynamic factor as a function of the transmitted loads for three different speeds. There is only a small decrease in dynamic factor with increased applied load.

Fig. 8 shows the effect of damping on the dynamic load. It is seen that damping has its greatest effect near resonance frequencies.

Changes in shaft stiffness have a minor effect on the system dynamic response. However changes of tooth stiffness have a major effect on the response. Fig. 9 shows that the higher the tooth stiffness the lower the dynamic response (dynamic factor). This is consistent with observations that as the tooth

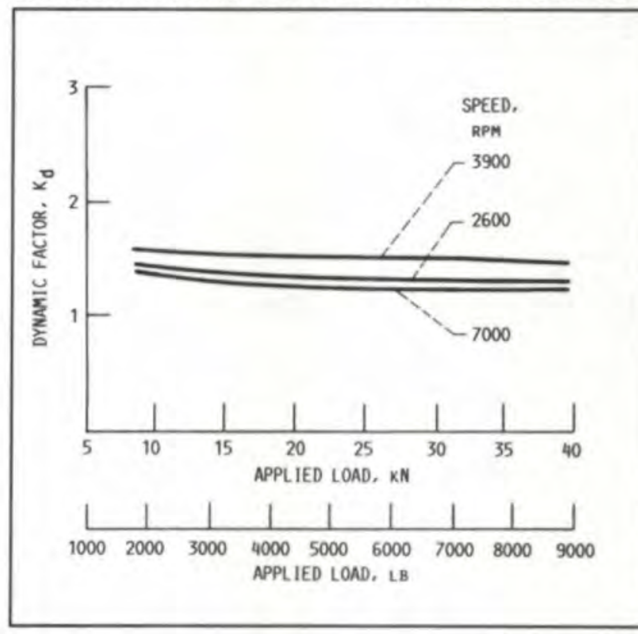

Fig. 7 – Effect of applied load on dymanic response.

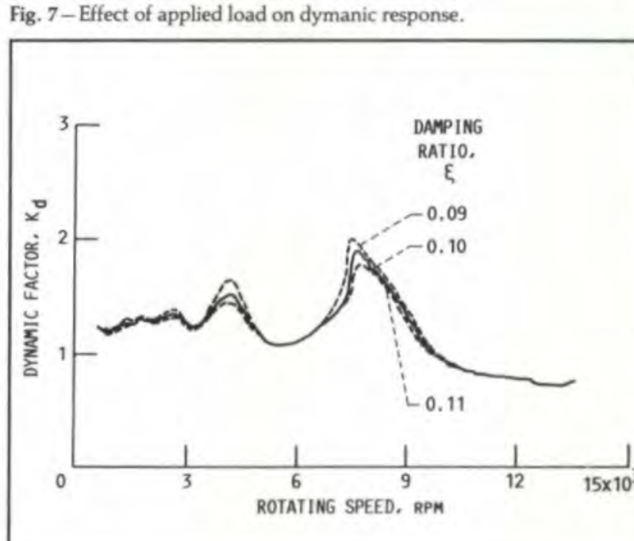

Fig. 8 – Effect of damping on dynamic response.

stiffness increases the effect of gear mass on the system dynamics is reduced. Fig. 9 also shows that system resonance frequencies are increased as the tooth stiffness increases. This is a potentially useful effect for the design of gear systems.

The effect of shaft mass is assumed small compared to that of the gears. Fig. 10 shows that as the gear inertia is reduced, the dynamic response is also reduced.

For gears with different diametral pitches, the dynamic response is different due to the change in contact ratio. Gears with a finer pitch have a higher contact ratio. Since the contact ratio is a measure of the duration of the load being shared by more than one pair of teeth, it has a significant effect on the system dynamic response.

Fig. 11 shows a comparison between gears having different diametral pitches. The finer pitch gears, having a higher contact ratio, have a smaller dynamic load than the coarser pitch gears.

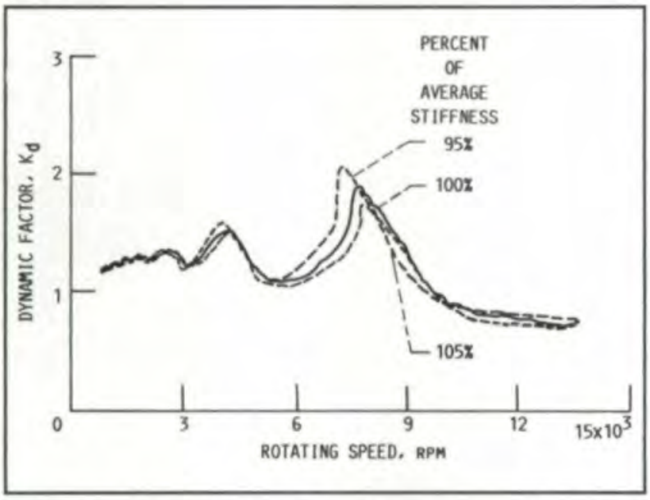

Fig. 9 – Effect of average tooth stiffness on dynamic response. Average tooth stiffness: 100% value = 3.991×10^5 N-m/rad.

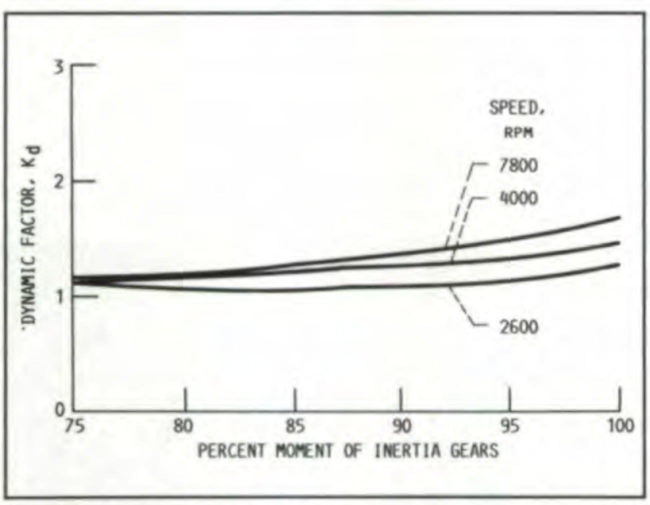

Fig. 10 – Effect of gear inertia on dynamic response. (Gear inertia: 100% value = 3.33×10^{-3} kg$-$m^2).

CIMA USA YOUR SOURCE FOR WORLD CLASS GEARMAKING TECHNOLOGY...

... lets you select familiar component systems

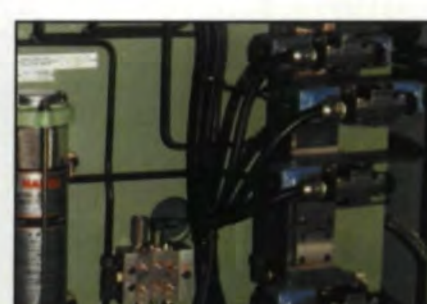

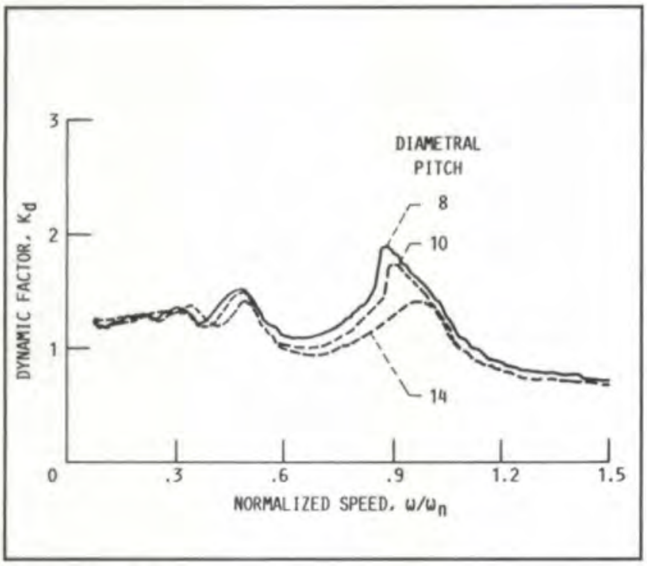

Fig. 11 – Effect of diametral pitch on dynamic response.

Discussion

In 1927, A.A. Ross[3] introduced the following empirical formula for the dynamic factor k_v:

$$k_v = \frac{78}{(78 + \sqrt{v})} \qquad (9)$$

where v is the pitch line speed measured in ft/min. This expression received acceptance as a standard factor used by the American Gear Manufacturer's Association (AGMA). In 1959, a similar factor for use with higher precision gears was introduced by Wellauer.[4]

$$k_v = \left[\frac{78}{78 + \sqrt{v}}\right]^{1/2} \qquad (10)$$

Equations 9 and 10 are recognized as being conservative when applied with very high precision gears. They are thought to predict dynamic loads which are higher than the actual loads.

Buckingham[5] has also developed an expression for the dynamic load in terms of the pitch line speed and the applied load. His formula is

$$W_d = W + [f_a(2f_b - f_a)]^{1/2} \qquad (11)$$

where W_d is the dynamic load, W is the applied load, and the factors f_a and f_b are

$$f_a = f_b f_c/(f_b + f_c) \text{ and } f_b = 0.0000555\,EF + W \qquad (12)$$

where F is the face width, E is the elastic constant, and f_c is

$$f_c = 0.00120\,[(R_1 + R_2)/R_1R_2]mv^2 \qquad (13)$$

where R_1 and R_2 are the pitch radii of the gears, and m is their effective mass. (In these expressions the units are in pounds and inches except for the pitch line speed which is measured in ft/min.)

Kubo[6] measured static and dynamic gear stresses on several high-precision spur gear systems. Kubo expressed the dynamic factor as the ratio of maximum dynamic to the maximum static stress. Since stress is proportional to load, Kubo's definition of dynamic factor is identical to that used here. Fig. 12 shows a comparison of $(1/K_v)$ from the AGMA high-precision formula (Equation 10), (W_d/W) from Buckingham's formula, Kubo's results, and the results of the computer simulation for an identical spur gear pair with 4 mm module, 25 teeth, 20° pressure angle, 15 mm face width, 131.5 kN/m applied load, and 207 GPa Young's modulus.

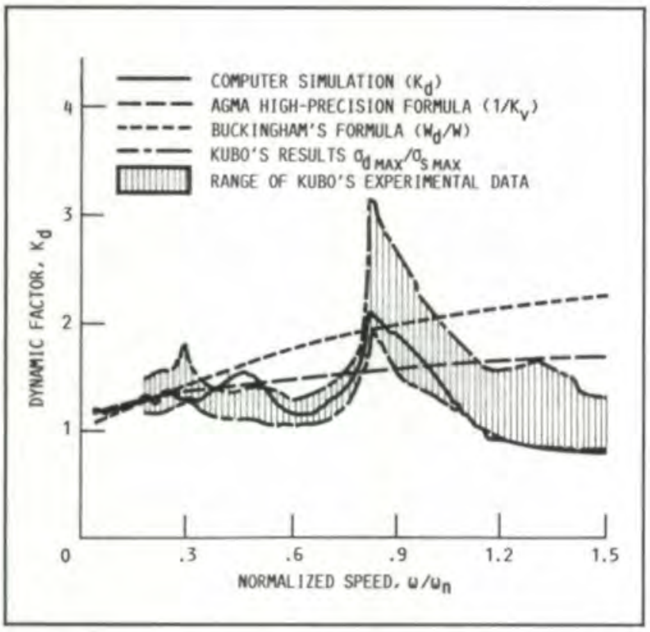

Fig. 12 – Comparison of experimental, empirical, and computer simulation results.

There is a good agreement between Kubo's result and the computer simulation.

Conclusions

From the foregoing results several conclusions may be stated:

1. For accurately made gears, the dynamic load is significantly affected by the contact ratio: for increased diametral pitch, that is, for high contact ratio gears, the dynamic load is decreased.

2. The tooth stiffness has a significant effect upon the dynamic load: the higher the stiffness, the lower the dynamic load. Also, the higher the stiffness, the higher the critical speed for peak response.

3. The dynamic load generally increases with the operating speed until a resonance is reached. The dynamic load decreases rapidly beyond the resonance.

4. Damping and friction decrease the dynamic load with the most dramatic effects occurring near the resonance frequencies.

5. The applied load has a relatively minor effect upon the dynamic factor.

6. Tooth separation – leading to impact – occurs in the double tooth contact region since the deflections are smallest in that region.

7. The dynamic factor is largest for contact points near the tooth tip.

8. The dynamic factor decreases with decreases in the gear body inertia. Shaft moment of inertia has a minimal effect upon the dynamic factor.

References:

1. LIN, H.H., HUSTON, R.L., and COY J.J. "On Dynamic Loads in Parallel Shaft Transmissions. I - Modeling and Analysis." NASA TM-100180, 1987. Also *Gear Technology*, Vol. 7, No. 1, Jan/Feb, 1990.
2. NAFEH, A.H. and MOOK, D.T. *Nonlinear Oscillations*. Wiley, 1979, Chapt. 5.
3. ROSS, A.A. "Tooth Pressures for High-Speed Gears." *Machinery* (NY), Vol. 34, No. 2, Oct. 1927, pp. 110-112.
4. WELLAUER, E.J. "An Analysis of Factors Used for Strength Rating of Helical Gears." *J. Eng. Ind.*, Vol. 82. No. 3, Aug. 1960, pp. 205-212.
5. BUCKINGHAM, E. *Analytical Mechanics of Gears*. Dover, 1963.
6. KUBO, A. "Estimation of Gear Performance." *Proceedings of the International Symposium on Gearing and Power Transmissions*. Japan Society of Mechanical Engineers, Tokyo, 1981, pp. 201-206.

Acknowledgements: Published in *ASME Journal of Mechanisms, Transmissions, and Automation in Design*, Vol 110, No. 2, June, 1988, pp. 221-229, and as NASA Technical Memorandum 100281 and AVSCOM T.M. 87-C-3. Reprinted with permission.

The Geometric Design of Internal Gear Pairs

J. R. Colbourne,
University of Alberta
Edmonton, Alberta, Canada

Abstract:

The paper describes a procedure for the design of internal gear pairs, which is a generalized form of the long and short addendum system. The procedure includes checks for interference, tip interference, undercutting, tip interference during cutting, and rubbing during cutting.

Introduction

The geometric design of any gear pair involves the selection of several quantities, including the tooth numbers, the module, the pressure angle, the tooth thicknesses, and the diameters of the gear blanks. After values have been chosen for each of these quantities, the design must be checked to ensure that certain requirements are met. There must be a suitable amount of backlash and adequate values for the contact ratio, the working depth, and the clearances. There must be no interference, and, whenever possible, undercutting should be avoided. In the case of an internal gear pair, there are several other checks to be made which do not apply to external gear pairs. There must be no tip interference, and it must be possible to cut the internal gear without tip interference from the cutter or rubbing during the return strokes of the cutter.

If all the design quantities are chosen independently, a long trial and error process is often required before optimum values are found. This paper describes a systematic procedure, in which the values of the design quantities are calculated in a specified order, to satisfy some of the necessary requirements. There is one free parameter left undetermined, and this is chosen by the designer to meet as far as possible the remaining requirements for the gear pair. The method can be regarded as a generalized form of the long and short addendum system.

The design procedure consists of the following steps. First, the module and the tooth numbers are selected so that the required ratio is obtained, and the standard center distance C_s is equal to or slightly less than the actual center distance C. Then the tooth thicknesses are chosen to give the specified backlash. This is the point where the free parameter is introduced, as we will see later in the paper. Assuming we know the specification of the cutter which will be used to cut the gears, the dedendum of each gear is effectively determined by the choice of the tooth thicknesses.

We now have to choose the addendum values for each gear. It is generally recognized that interference in internal gear pairs is most likely to occur at the tooth fillets of the pinion, and it is, therefore, common practice to shorten the teeth of the internal gear to prevent the possibility of interference. One effect of the shorter teeth is that the working depth in the gear pair is often less than two modules, the value generally recommended for external gear pairs. However, the contact ratio is usually still quite adequate, in spite of the smaller working depth, due to the manner in which the teeth of the internal gear wrap around the path of contact. With these considerations in mind, we choose the addendum values of the two gears in a manner that first avoids interference at the tooth fillets of the pinion, and then maximizes the working depth. This paper contains the equations necessary to carry out each step of the design procedure and also to apply the checks described earlier.

In the design of internal gear pairs, it is possible to use very large values of profile shift. This is not the case for external gear pairs, where an increase in the profile shift of one gear must be accompanied by a decrease in that of the other in order to maintain the necessary backlash. The sum of the profile shift values in an external gear pair is essentially determined by the value of $(C-C_s)$, the amount by which the center distance is extended from its standard value, and this quantity is limited by the maximum value permitted for the operating pressure angle. For this reason, it is very unusual for either gear in an external gear pair to have a profile shift of more than one module. The situation in an internal gear pair is different. When the profile shift of the pinion is increased, the profile shift of the internal gear must also be increased if the backlash is to remain unchanged. The increases only reach their limit when the teeth of the internal gear become weaker than those of the pinion, and this generally does not happen until the profile shift values are quite large. It is, therefore, possible for both the pinion and the internal gear to have profile shift values of considerably more than one module. The advantage of these large profile shift values is that they can sometimes be used to prevent tip interference and the other problems discussed earlier.

AUTHOR:

JOHN R. COLBOURNE *is a professor of Mechanical Engineering at the University of Alberta, where he teaches and does research on the geometry and tooth strength of gears. He is the author of the book,* The Geometry of Involute Gears, *and has also worked as a consultant to the gear industry. Dr. Colbourne received his bachelor's degree from Cambridge University, England, and his doctorate from Stanford University, Stanford, CA.*

Terminology, Notation, and Some Well-Known Results

The pitch circle of a gear when it is meshed with its basic rack will be called the standard pitch circle, and all quantities defined on this circle will be identified by the subscript s. The pitch circles of two gears in operation, often called the operating pitch circles, will be called simply the pitch circles, and quantities defined on these circles will be identified by the subscript p. The subscripts R and b will apply to the same quantities at a typical radius R and at the base circles.

Equations 1-9 are presented without proof, since they are well known. For a gear with N teeth, module m and pressure angle ϕ_s, Equations 1 and 2 give the radii R_s and R_b of the standard pitch circle and the base circle. Equations 3-5 give the profile angle ϕ_R, the polar coordinate θ and the tooth thickness t_R, all measured at radius R. For an internal gear pair, Equations 6-9 give the pitch circle radii, the operating circular pitch p_p, and the operating pressure angles ϕ of the gear pair and ϕ_p of each gear. Where there are alternative signs in Equations 4 and 5, the upper sign refers to the pinion, and the lower sign refers to the internal gear. In Equations 6-9, and throughout this paper, the pinion is numbered as gear 1 and the internal gear as gear 2.

$$R_s = \frac{1}{2} N m \tag{1}$$

$$R_b = R_s \cos \phi_s \tag{2}$$

$$\phi_R = \arccos \frac{R_b}{R} \tag{3}$$

$$\theta = \pm \frac{t_s}{2R_s} + (\operatorname{inv} \phi_s - \operatorname{inv} \phi_R) \tag{4}$$

$$t_R = R \left[\frac{t_s}{R_s} \pm 2(\operatorname{inv} \phi_s - \operatorname{inv} \phi_R) \right] \tag{5}$$

$$R_{p1} = \frac{N_1 C}{(N_2 - N_1)} \tag{6}$$

$$R_{p2} = \frac{N_2 C}{(N_2 - N_1)} \tag{7}$$

$$p_p = \frac{2\pi C}{(N_2 - N_1)} \tag{8}$$

$$\phi = \phi_p = \arccos \frac{(R_{b2} - R_{b1})}{C} \tag{9}$$

The Design Procedure

The tooth thicknesses of the pinion and the internal gear at their pitch circles must be chosen in a manner which gives the specified value for the backlash B. This requirement can be met by the following values,

$$t_{p1} = \frac{1}{2} (p_p - B) + \Delta t_p \tag{10}$$

$$t_{p2} = \frac{1}{2} (p_p - B) - \Delta t_p \tag{11}$$

The quantity Δt_p in these equations is the free parameter that was mentioned earlier. Its value, which may be positive or negative, is chosen by the designer, and we will discuss later the effects of a change in the value of Δt_p.

Once the tooth thicknesses are chosen, and assuming that we know the specification of the cutter, it is possible to calculate the radii of the two root circles. In other words, the dedendum of each gear is known. Details of these calculations are given in the Appendix. We also show in the Appendix, how to calculate the radii R_{f1} and R_{f2} of the fillet circles, which pass through the tops of the tooth fillets, and the radii R_{L1} and R_{L2} of the limit circles.

We now choose the radius R_{T2} of the internal gear tip circle so that the pinion limit circle radius is 0.025 modules larger than the fillet circle radius,

$$R_{L1} = R_{f1} + 0.025m \tag{12}$$

$$R_{T2}^2 = R_{b2}^2 + [(R_{b2} - R_{b1})\tan\phi + \sqrt{(R_{L1}^2 - R_{b1}^2)}]^2 \tag{13}$$

The second of these equations is a rearrangement of Equation A19 in the Appendix. By choosing R_{T2} according to this equation, we are designing the gear pair so that the form circle of the pinion passes exactly through the tops of its tooth fillets, and we have thereby insured that there will be no interference at the pinion tooth fillets. If the clearance at the pinion root circle is less than 0.25 modules, the teeth of the internal gear should be shortened until the required minimum clearance is achieved. The radius of the tip circle is then given by the following equation,

$$R_{T2} = C + R_{root,1} + 0.25m \tag{14}$$

We also have to choose a value for the radius R_{T1} of the pinion tip circle. In order to obtain the maximum available working depth, we choose R_{T1} so that the clearance at the root circle of the internal gear is equal to the minimum acceptable value,

$$R_{T1} = R_{root,2} - C - 0.25m \tag{15}$$

Interference

The design procedure has already guaranteed that there will be no interference at the tooth fillets of the pinion. To insure that there is also no interference at the tooth fillets of the internal gear, we want the limit circle radius of the internal gear to be smaller than that of its fillet circle by at least 0.025 modules,

$$R_{L2} \le R_{f2} - 0.025m \tag{16}$$

Expressions for R_{L2} and R_{f2} are given in the Appendix. This condition is generally satisfied for most normal designs, and in cases where it is not, the interference can almost always be eliminated by an increase in Δt_p.

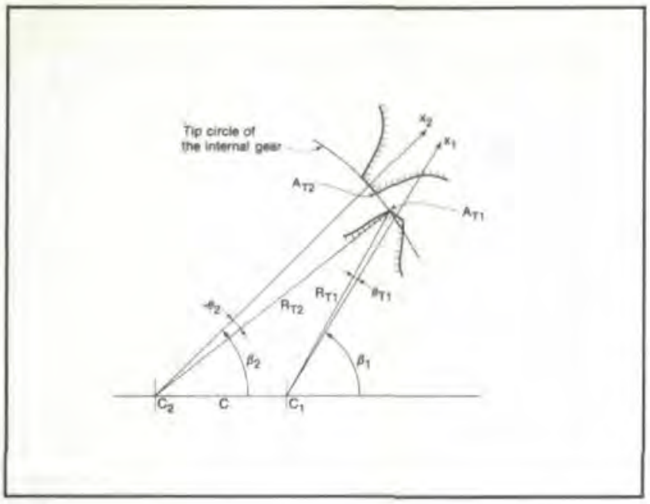

Fig. 1

Tip Interference

Tip interference occurs when the tooth tips collide as the teeth are passing in and out of mesh. Fig. 1 shows a gear pair in position with the tooth tip A_{T1} of the pinion lying exactly on the tip circle of the internal gear. To prevent tip interference, there must be an adequate clearance between the tooth tips in this position.

In each gear, we construct coordinate systems with the x_1 and x_2 axes coinciding with tooth center-lines, and the positions of the gears are defined by the counterclockwise angles β_1 and β_2 through which these axes have rotated from the line of centers. We also use polar coordinates in each gear, with the angles θ being measured counterclockwise from the x axes. The angles θ_{T1} and θ_{T2} of the tooth tip points A_{T1} and A_{T2} are found by means of Equations 3 and 4. In Fig. 1, the polar angle of point A_{T1} relative to the x_2 axis is shown as θ_2, and its value is not yet known.

The value of β_1 can be found by applying the cosine rule to triangle $C_1C_2A_{T1}$ in Fig. 1,

$$\beta_1 = \arccos\left[\frac{R_{T2}^2 - C^2 - R_{T1}^2)}{2CR_{T1}}\right] - \theta_{T1} \qquad (17)$$

As the gears rotate, there is obviously a relation between β_1 and β_2. To determine this relation, we first consider the gears when there is contact at the pitch point, so that β_1 and β_2 have the values $(-t_{p1}/2R_{p1})$ and $(t_{p2}/2R_{p2})$. Any rotations from this position must be in the ratio $R_{p2}:R_{p1}$, so we obtain the general relation between β_1 and β_2,

$$R_{p1}\beta_1 - R_{p2}\beta_2 + \frac{1}{2}(t_{p1} + t_{p2}) = 0 \qquad (18)$$

Having found β_1 from Equation 17, we now use Equation 18 to calculate β_2. We then return to triangle $C_1C_2A_{T1}$ in Fig. 1, and use the sine rule to calculate θ_2.

$$\theta_2 = \arcsin\left[\frac{R_{T1}}{R_{T2}}\sin(\beta_1 + \theta_{T1})\right] - \beta_2 \qquad (19)$$

The arc distance between A_{T2} and A_{T1} is equal to $R_{T2}(\theta_{T2} - \theta_2)$, where the two angles are expressed in radians. To prevent the possibility of tip interference, this distance should be not less than some specified value, such as 0.05 modules.

$$R_{T2}(\theta_{T2} - \theta_2) \geq 0.05m \qquad (20)$$

Undercutting

The involute tooth profile of an internal gear can only be cut by the involute part of the cutter teeth. There will be undercutting at the tooth tips of the gear if the contact point moves down the cutter teeth to a point below the base circle. If the cutter teeth have fillets extending outside the base circle, then the contact between the gear and the cutter should end before the contact point reaches the cutter fillet circle.

This condition implies that the contact path during cutting must end above F_c, the point where the fillet circle of the cutter intersects the common tangent to the base circles. We can then read from Fig. 2 the minimum value for the tip circle radius of the internal gear,

$$(R_{T2}^2)_{min} = R_{b2}^2 + [(R_{b2} - R_{bc})\tan\phi^c + \sqrt{(R_{fc}^2 - R_{bc}^2)}]^2 \qquad (21)$$

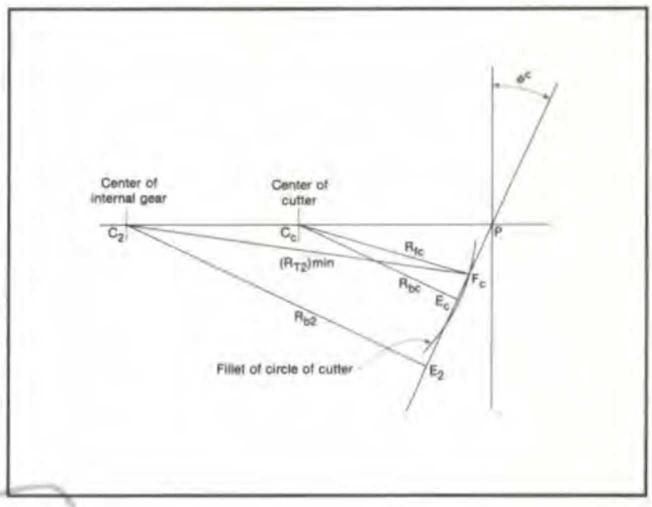

Fig. 2

In this equation, quantities on the cutter are indicated by the subscript c, and ϕ^c is the cutting pressure angle, whose value is given by the equations in the Appendix. R_{fc} is the fillet circle radius of the cutter, which must be measured. If the value is not known when the gear pair is designed, we can replace R_{fc} by R_{bc}, and Equation 21 will then only insure that the path of contact ends above the cutter interference point E_c.

In certain circumstances, it may be advantageous to use a cutter that does not satisfy Equation 21. If the teeth of the internal gear are to be cut with tip relief, this can be achieved by allowing the tooth fillets of the cutter to cut part of the gear tooth profiles. Equation 21 will then give the radius at which the tip relief begins.

Tip Interference During Cutting

We have already discussed the possibility of tip interference during the operation of an internal gear pair. The same phenomenon may occur when the internal gear is being cut, but, of course, in this case the result is that part of the involute profiles of the gear teeth are removed. In other words, tip interference during cutting is another form of undercutting.

Tip interference may occur either when the cutter reaches its full depth or at some time when the cutter is being fed in. We therefore need to consider the possibility of tip interference when the cutting center distance is at any value C_f (the feed-in center distance), which is either less than or equal to the final cutting center distance C^c. Tip interference will occur if A_{hc}, the end point of the involute section of the cutter tooth, passes through the tooth of the internal gear. The coordinates (R_{hc}, θ_{hc}) of point A_{hc} are given in the Appendix. The equations giving the conditions for no tip interference are essentially the same as Equations 17-20, with the pinion replaced by the cutter.

$$\beta_c = \arccos\left[\frac{(R_{T2}^2 - C_f^2 - R_{hc}^2}{2C_f R_{hc}}\right] - \theta_{hc} \qquad (22)$$

$$R_{sc}\beta_c - R_{s2}\beta_2 + \frac{1}{2}\pi m = 0 \qquad (23)$$

$$\theta_2 = \arcsin\left[\frac{R_{hc}}{R_{T2}}\sin(\beta_c + \theta_{hc})\right] - \beta_2 \qquad (24)$$

$$R_{T2}(\theta_{T2} - \theta_2) \geq 0.02m \qquad (25)$$

Equation 23 is derived from Equation 18 in the following manner. There is no backlash during the cutting process, so the sum of the tooth thicknesses is equal to the circular pitch, all measured at the cutting pitch circles. Equation 18 is then multiplied by the ratio (C_s^c/C^c), where C_s^c is the standard cutting center distance, to obtain Equation 23.

The suggested minimum clearance between the path of A_{hc} and the gear tooth tip A_{T2} is only 0.02 modules, which is less than the value 0.05 modules in Equation 20. The lower value was chosen because the tolerances are closer during cutting than in operation, and also because the problems caused by a small amount of tip interference during cutting are much less severe than problems caused by tip interference in operation.

Cutting begins when the cutting center distance is equal to $(R_{T2} - R_{Tc})$ and ends when the cutting center distance reaches its final value C^c. Equations 22-25 should be checked for several values of C_f between these two limits to insure that there is no tip interference at any time during the cutting process.

Rubbing

During the return strokes of the cutter, the workpiece and the cutter must be separated to prevent them rubbing together. If rubbing occurs, it causes burrs on the workpiece and excessive wear on the cutter. To achieve the required separation, either the workpiece or the cutter, depending on the design of the machine, must be displaced a small distance away from the other. It is the purpose of this section of the article to determine whether such a displacement , which will prevent the rubbing, can be made and in what direction it should be made. In order to be specific, we will discuss the case when the cutter is displaced. Obviously, if in fact the workpiece is displaced, the direction must be in the opposite direction to the one we determine for the cutter.

Fig. 3 shows the gear blank and the cutter at the instant when point A_{hc}, the end point of the involute section on the trailing profile of a cutter tooth, is just crossing the tip circle of the gear blank. The tangent to the cutter tooth profile makes an angle α with the line of centers, whose value can be read from diagram,

$$\alpha = \arccos\frac{[R_{T2}^2 - (C^c)^2 - R_{hc}^2]}{2C^c R_{hc}} - \phi_{hc} \qquad (26)$$

In order to create a gap between the trailing profile of the cutter tooth and the workpiece, the displacement must be in a direction which makes an angle greater than α with the line of centers. Also in Fig. 3, the leading profiles of the cutter teeth touch the workpiece, and the common tangents make an angle ϕ^c with the line of centers. In this case, a displacement which creates a gap between the two profiles must be

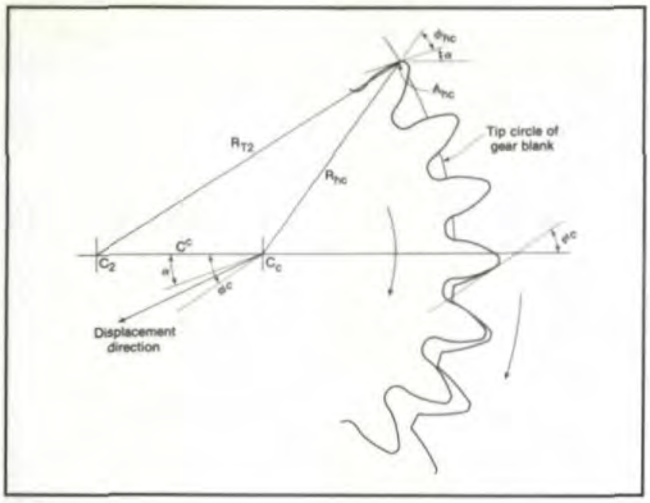

Fig. 3

at an angle with the line of centers, which is less than ϕ^c. For these two conditions to be possible, the angle α given by Equation 26 must be smaller than ϕ^c by at least a few degrees, and the direction of the displacement must be chosen between α and ϕ^c, as shown in Fig. 3.

Since there is only one position where the common tangent makes an angle α with the line of centers, whereas there are several positions where the angle is ϕ^c, it is preferable for the displacement direction to be chosen closer to α than to ϕ^c. It is, therefore, suggested that the displacement direction should split the angle in the ratio 1:2.

$$\text{Displacement direction} = \frac{2}{3}\alpha + \frac{1}{3}\phi^c \qquad (27)$$

We have not yet discussed the minimum value of $(\phi^c - \alpha)$ required to avoid rubbing, but we will return to this question later in the article.

Design Examples

The design equations given in this paper, together with all the checks, can be programmed for a desk computer, with Δt_p as one of the inputs to the program. Whenever one of the checks is not satisfactory, the designer can try altering the value of Δt_p, until the required condition is satisfied. In most cases, an increase of Δt_p is called for. If all the checks are satisfactory, then the value of Δt_p may still be modified, in a manner that brings the tooth strength of the pinion into balance with that of the gear.

Over the years, a number of design rules have come into existence for the purpose of avoiding problems such as tip interference or rubbing. These rules give values for the minimum difference between the tooth numbers, either of the pinion and gear or of the cutter and gear. However, as we have shown, the occurrence of interference, tip interference, rubbing, etc., depends on many quantities, including in particular the center distance, the tip circle radii, and the amounts of profile shift. It is believed by the author that there are no simple rules which are invariably accurate, and it is therefore better to carry out the checks for each gear pair design. To emphasize this point, the two design examples presented here will be ones that break every existing rule, but are nevertheless believed to be satisfactory designs. In the first design, the difference between the tooth numbers of the pinion and gear is only 5, while in the second example, the internal gear is cut by a cutter which has only 8 teeth less than the gear. It is not suggested that the design procedure can only be used for unorthodox designs. On the contrary, the method will give good designs when there are no unusual requirements. But it will also sometimes give satisfactory designs in cases when, according to the existing design rules, no design is possible.

Example 1

A pinion cutter has 20 teeth, module 6mm, pressure angle ϕ_s of 20°, tooth thickness t_{sc} of 9.425, tip circle radius R_{Tc} of 67.5, and tooth tip rounding radius r_{cT} of 1.5. The cutter is to be used to cut an internal gear pair with the following specification: $N_1 = 29$, $N_2 = 34$, $C = 15.57$, $B = 0.36$. Complete the design, using the value 1.692 for Δt_p, and check that there is no tip interference.

On each line of the design examples, the number in brackets gives the equation used to calculate the stated value. All lengths are expressed in mms.

	Cutter data	
R_{sc}	= 60.0	(1)
R_{bc}	= 56.382	(2)
R'_c	= 66.0	(A1)
ϕ_{hc}	= 32.421°	(A2)
R_{hc}	= 66.792	(A3)
θ_{hc}	= 1.385°	(A4)
	Design of the gears	
R_{s1}	= 87.0	(1)
R_{s2}	= 102.0	(1)
R_{b1}	= 81.753	(2)
R_{b2}	= 95.849	(2)
ϕ_p	= 25.137°	(9)
R_{p1}	= 90.306	(6)
R_{p2}	= 105.876	(7)
t_{p1}	= 11.295	(10)
t_{p2}	= 7.911	(11)
t_{s1}	= 13.595	(5)
t_{s2}	= 4.440	(5)
$\phi_1^c = \phi_{p1}^c$	= 24.764°	(A16, A9, A10)
$\phi_2^c = \phi_{p2}^c$	= 33.108°	(A8, A9, A10)
C_1^c	= 152.124	(A17)
C_2^c	= 47.117	(A12)
$R_{root,1}$	= 84.624	(A18)
$R_{root,2}$	= 114.617	(A13)
R_{f1}	= 86.387	(A21)
R_{L1}	= 86.537	(12)
R_{T2}	= 102.035	(13)
R_{T1}	= 97.547	(15)

With a difference between the tooth numbers of the gear and pinion of only five, it is obvious that there is a danger of tip interference. The value chosen for Δt_p was the lowest value for which there is no tip interference, according to Equation 20, and this value was found by trial and error. We now confirm that Equation 20 is indeed satisfied.

$$\begin{aligned} \theta_{T1} &= 1.097° && (3,4) \\ \beta_1 &= 76.484° && (17) \\ \beta_2 &= 70.433° && (18) \\ \theta_2 &= -1.423° && (19) \\ \theta_{T2} &= -1.254° && (3,4) \\ \text{Clearance} &= R_{T2}(\theta_{T2} - \theta_2) = 0.301 \text{ mm} \end{aligned}$$

Since the clearance is greater than 0.05 modules, which is 0.300 mm, there will be no tip interference. The gear pair is shown in Fig. 4, where it can be seen that the clearance is just sufficient.

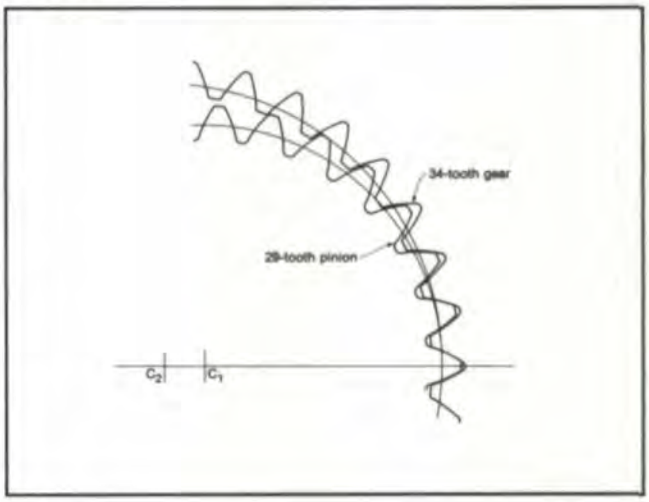

Fig. 4

Example 2

The cutter described in Example 1 is to be used to cut a gear pair with the following specification: $N_1 = 21$, $N_2 = 28$, $C = 21.30$, $B = 0.36$. Complete the design, using $\Delta t_p = 2.322$, and check that there is no tip interference or rubbing during cutting.

R_{s1}	= 63.0	(1)
R_{s2}	= 84.0	(1)
R_{b1}	= 59.201	(2)
R_{b2}	= 78.934	(2)
ϕ_p	= 22.111°	(9)
R_{p1}	= 63.900	(6)
R_{p2}	= 85.200	(7)
t_{p1}	= 11.701	(10)
t_{p2}	= 7.057	(11)
t_{s1}	= 12.225	(5)
t_{s2}	= 6.040	(5)
$\phi_1^c = \phi_{p1}^c$	= 23.983°	(A16, A9, A10)
$\phi_2^c = \phi_{p2}^c$	= 34.534°	(A8, A9, A10)
C_1^c	= 126.504	(A17)
C_2^c	= 27.377	(A12)
$R_{root,1}$	= 59.004	(A18)
$R_{root,2}$	= 94.877	(A13)
R_{f1}	= 61.224	(A21)
R_{L1}	= 61.374	(12)
R_{T2}	= 82.562	(13)
R_{T1}	= 72.077	(15)

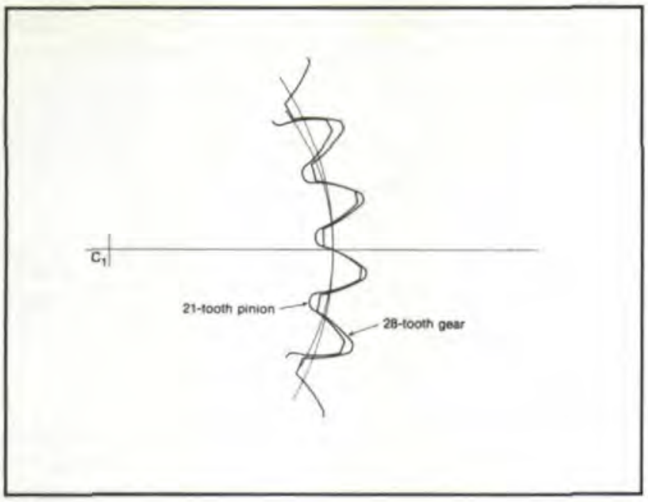

Fig. 5

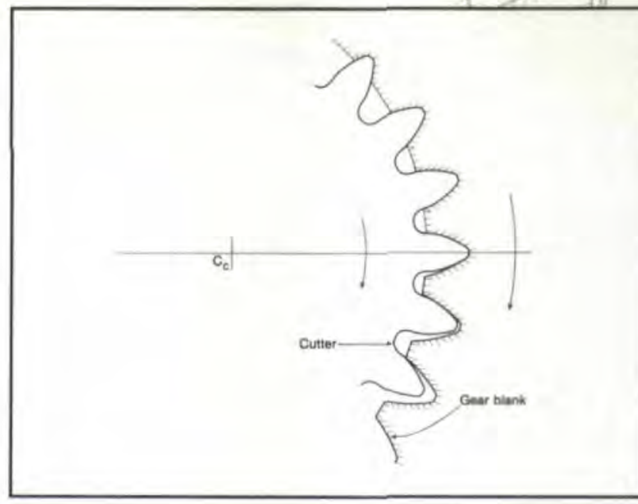

Fig. 6

The design is now complete, and the gear pair is shown in Fig. 5. We finish the example by showing the checks for tip interference and rubbing during cutting.

The cutting begins when the center distance is 15.062 mm, and ends when it is 27.377 mm. As a typical check for tip interference during cutting, we consider the case when the cutting center distance is midway between these values.

$$C_f = 21.219$$
$$\beta_c = 46.386^\circ \qquad (22)$$
$$\beta_2 = 39.561^\circ \qquad (23)$$
$$\theta_2 = -2.761^\circ \qquad (24)$$
$$\theta_{T2} = -1.727^\circ \qquad (3,4)$$
$$\text{Clearance} = R_{T2}(\theta_{T2}-\theta_2) = 1.490 \text{ mm}$$

The clearance is more than adequate, and we would find that the same is true at other values of C_f. We now check for rubbing.

$$\alpha = 31.533^\circ \qquad (26)$$

The cutting pressure angle ϕ_2^c is larger than α by 3°. The reason for this particular result is that Δt_p was chosen, again by trial and error, as the smallest value which would give a margin of 3°. We must now determine whether this value of $(\phi_2^c-\alpha)$ is large enough.

Fig. 6 shows the cutter and the partly finished gear blank of Example 2. In the upper half of the diagram, the cutter teeth are penetrating into the gear blank, so that at this stage the tooth spaces in the gear blank are essentially the same shape as the cutter teeth. In the lower half of the diagram, the cutter teeth are receding from the gear blank, and the tooth spaces have attained their final shape.

Between the beginning of a cutting stroke and the end of the return stroke, the cutter will rotate through a small angle $\Delta\beta_c$, and the gear blank will rotate through a corresponding angle $\Delta\beta_2$. If cutting could take place during the return stroke, the cutter would penetrate a certain distance into the gear blank, and it is this overlap between the positions of the cutter and the gear blank which causes the rubbing on the return strokes. The cutter back-off displacement must move the cutter to a position where there is no overlap.

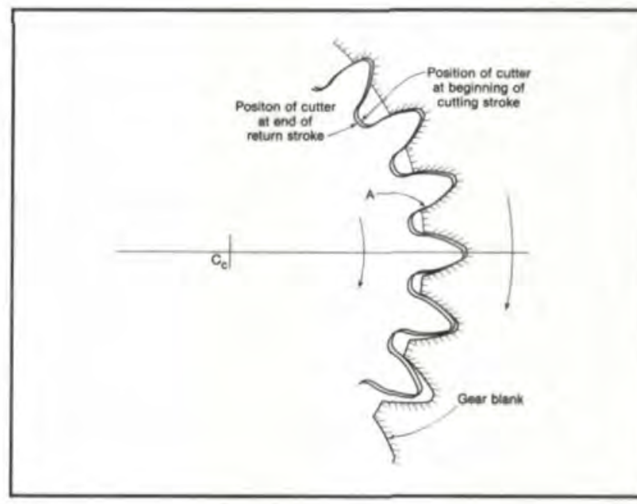

Fig. 7

Fig. 7 is the same as Fig. 6, except that the cutter is also shown in its displaced position, which was found in the following manner. From the time when the cutter was in the position shown as the cutting position, it is assumed that the cutter rotates 0.500° clockwise, the gear blank rotates 0.357° clockwise, and the cutter is displaced a distance 1.2 mm at an angle 32.533° with the line of centers. The new position of the cutter relative to the gear blank is then found by rotating the entire gear pair 0.357° counterclockwise about the center of the gear, and this position is shown in the diagram as the return stroke position. The rotation of 0.5° represents 720 strokes per revolution, which is a typical rate, and the displacement of 1.2 mm is larger than normal, but was chosen so that the new position can be clearly seen in the diagram.

It is evident from the diagram that there is no overlap between the gear blank and the displaced position of the cutter, except perhaps at the point labelled A. The cutter tooth has been displaced, at the angle given by Equation 27, along a finished section of the gear tooth profile. In order to determine whether there is any overlap, we express the displacement direction in the form $(\phi_2^c-\delta)$, and we replace the tooth profiles with circular arcs whose radii are equal to the radii of curvature of the teeth, as shown in Fig. 8.

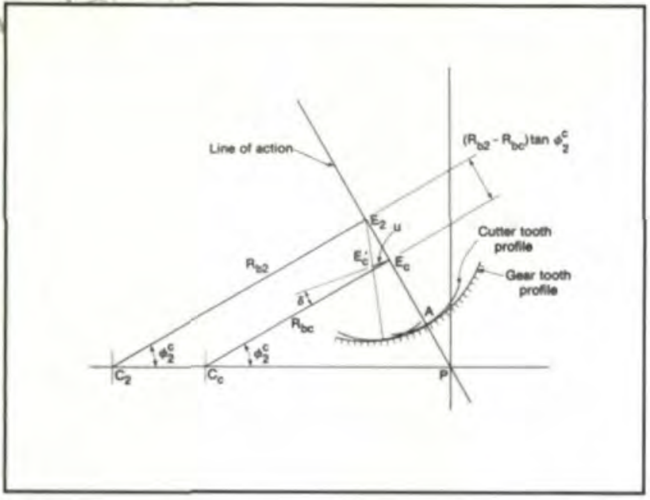

Fig. 8

The center of curvature of the cutter tooth is at E_c, the point where the common normal touches the base circle. If there is to be exactly no overlap after the displacement, E_c will move to E_c', the same distance from the gear tooth profile. The angle δ (measured in radians) and the displacement u are then approximately related as follows,

$$\delta = \frac{u}{2(R_{b2} - R_{bc}) \tan \phi_2^c} \tag{28}$$

This equation gives the minimum value of δ to avoid rubbing. When the displacement direction is chosen according to Equation 27, the angle δ is equal to $2(\phi_2^c - \alpha)/3$, and we, therefore, obtain a minimum value for $(\phi_2^c - \alpha)$. It is perhaps good practice to increase this minimum by a certain margin to allow for the errors in approximating the tooth shapes by circular arcs. If we increase it by one-third and convert from radians to degrees, we obtain the final minimum value for $(\phi_2^c - \alpha)$,

$$(\phi_2^c - \alpha)_{min} = \frac{180u}{\pi(R_{b2} - R_{bc}) \tan \phi_2^c} \tag{29}$$

Returning to Example 2, we now choose a value of 0.7 mm for the back-off displacement, which is more realistic than the 1.2 mm used for Fig. 7. Equation 29 then shows that 2.6° is the minimum value required for $(\phi_2^c - \alpha)$ to avoid rubbing, so the actual value of 3° is satisfactory.

In the discussion of this example, the general method has become somewhat obscured by the details of the example. In the design procedure, we simply choose a value for Δt_p, calculate the displacement direction by means of Equations 26 and 27, and then check that Equation 29 is satisfied to insure that there will be no rubbing.

Appendix

Because of space limitations, the explanations in this article are inevitably rather brief. The proofs in the Appendix and much of the material in the article, are described in more detail in Reference 1.

Pinion Cutter Tooth Tip Geometry

The tooth profile of a pinion cutter may coincide with the involute right out to the tip circle of the cutter, or it may be rounded at the tip. For cutting internal gears, it is preferable to use a cutter with rounded tooth tips, since this gives a larger radius of curvature at the root circle of the internal gear. We, therefore, consider a cutter in which the tooth tip is rounded with a radius r_{cT}. It is then necessary to find the coordinates of A_{hc}, the end point of the involute section of the tooth profile.

Fig. 9 shows a tooth of the cutter, and the center A'_c of the circular section at the tooth tip lies at radius R'_c. We use the diagram to write down two relations, which can be used to calculate the profile angle ϕ_{hc} at point A_{hc},

$$R'_c = R_{Tc} - r_{cT} \qquad (A1)$$

$$R_{bc} \tan \phi_{hc} = \sqrt{(R'^2_c - R^2_{bc})} + r_{cT} \qquad (A2)$$

The polar coordinates of point A_{hc} are then given by Equations 3 and 4,

$$R_{hc} = \frac{R_{bc}}{\cos \phi_{hc}} \qquad (A3)$$

$$\theta_{hc} = \frac{t_{sc}}{2R_{sc}} + (\text{inv}\,\phi_s - \text{inv}\,\phi_{hc}) \qquad (A4)$$

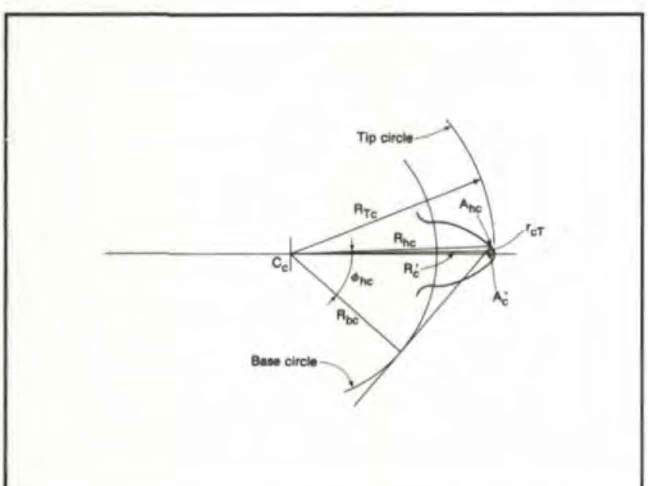

Fig. 9

Cutting Center Distance

In order to calculate the root circle radii on the pinion and the internal gear, it is necessary to find the cutting center distance for each gear. We consider first the case of the internal gear.

We know the tooth thickness t_{sc} of the cutter at its standard pitch circle. There is no backlash during the cutting process, so on the cutting pitch circles the tooth thickness of the gear is equal to the space width of the cutter.

$$t^c_{p2} = p^c_p - t^c_{pc} \qquad (A5)$$

The radii of the cutting pitch circles are given by Equations 6 and 7 in terms of the cutting center distance C^c_2.

$$R^c_{pc} = \frac{N_c C^c_2}{(N_2 - N_c)} \qquad (A6)$$

$$R^c_{p2} = \frac{N_2 C^c_2}{(N_2 - N_c)} \qquad (A7)$$

We use Equation 5 to express t^c_{p2} and t^c_{pc} in terms of the corresponding tooth thicknesses at the standard pitch circles.

$$R^c_{p2}\left[\frac{t_{s2}}{R_{s2}} - 2\,(\text{inv}\,\phi_s - \text{inv}\phi^c_{p2})\right]$$

$$= p^c_p - R^c_{pc}\left[\frac{t_{sc}}{R_{sc}} + 2(\text{inv}\,\phi_s - \text{inv}\,\phi^c_{p2})\right]$$

In this equation, ϕ^c_{p2} is the pressure angle of either the gear or the cutter at their cutting pitch circles. We multiply the entire equation by the ratio (C^c_{s2}/C^c_2), where C^c_{s2} is the standard cutting center distance, equal to $(R_{s2} - R_{sc})$, and we obtain an expression for inv ϕ^c_{p2},

$$\text{inv}\,\phi^c_{p2} = \text{inv}\,\phi_s - \frac{1}{2C^c_{s2}}\,(p_s - t_{s2} - t_{sc}) \qquad (A8)$$

To find the corresponding value of ϕ^c_{p2}, we make use of two equations in which the coefficients are simplified from a set developed by Polder[(2)], whose paper also contains much useful material on the limiting profile shift values in internal gear pairs.

$$q = (\text{inv}\,\phi^c_{p2})^{2/3} \qquad (A9)$$

$$\frac{1}{\cos \phi^c_{p2}} = 1.0 + 1.04004q + 0.32451q^2 - 0.00321q^3 - 0.00894q^4 + 0.00319q^5 - 0.00048q^6 \qquad (A10)$$

Finally, the cutting pressure angle ϕ^c_2 and the corresponding cutting center distance C^c_2 are given by Equation 9, and the root circle radius of the gear can then be found.

$$\phi^c_2 = \phi^c_{p2} \qquad (A11)$$

$$C^c_2 = \frac{(R_{b2} - R_{bc})}{\cos \phi^c_2} \qquad (A12)$$

$$R_{root,2} = C^c_2 + R_{Tc} \qquad (A13)$$

The method is the same when we calculate the cutting center distance for the pinion. There are sign changes in some of the equations, which are given below,

$$R_{pc}^{c} = \frac{N_c C_1^c}{(N_1+N_c)} \quad \text{(A14)}$$

$$R_{p1}^{c} = \frac{N_1 C_1^c}{(N_1+N_c)} \quad \text{(A15)}$$

$$\text{inv}\,\phi_{p1}^{c} = \text{inv}\,\phi_s + \frac{1}{2C_{s1}^{c}}\,(p_s - t_{s1} - t_{sc}) \quad \text{(A16)}$$

$$C_1^c = \frac{(R_{b1}+R_{bc})}{\cos\phi_1^c} \quad \text{(A17)}$$

$$R_{root,1} = C_1^c - R_{Tc} \quad \text{(A18)}$$

Limit Circle Radii

The meshing diagram for an internal gear pair is shown in Fig. 10. The path of contact lies on line E_1E_2, the common tangent to the base circles. The ends of the path of contact are at T_1 and T_2, the points where the tip circles intersect line E_1E_2. The circle in the pinion which passes through T_2, and the circle in the internal gear which passes through T_1, are known as the limit circles of the pinion and gear, because the active parts of the tooth profiles end at these circles. The radii of the two limit circles can be read from the diagram,

$$R_{L1}^2 = R_{b1}^2 + [\sqrt{(R_{T2}^2 - R_{b2}^2)} - (R_{b2}-R_{b1})\tan\phi]^2 \quad \text{(A19)}$$

$$R_{L2}^2 = R_{b2}^2 + [\sqrt{(R_{T1}^2 - R_{b1}^2)} + (R_{b2}-R_{b1})\tan\phi]^2 \quad \text{(A20)}$$

Fillet Circle Radii

The involute part of the gear tooth profiles are cut by the involute part of the cutter tooth. On both the pinion and the gear, the point where the involute ends and the fillet begins is cut by point A_{hc} on the cutter, whose coordinates were given by Equations A3 and A4. The circles in each gear through the end points of the fillets have been referred to in this paper as the fillet circles of the gears. They are customarily called the true involute form circles (or tif circles), but this name has not been used here, since there is a danger of confusion with the form circles, which are defined quite differently.

Figs. 11 and 12 show the meshing diagrams for the pinion and cutter and for the gear and cutter. In each diagram, the point where the path of A_{hc} intersects the common tangent to the base circles is labelled H_c, and this is the end of the cutting path of contact for the involute part of the gear tooth profile. The circle in each gear through point H_c is the fillet circle, and the radii of these two circles can be read from the diagrams.

$$R_{f1}^2 = R_{b1}^2 + [(R_{b1}+R_{bc})\tan\phi_1^c - \sqrt{(R_{hc}^2 - R_{bc}^2)}]^2 \quad \text{(A21)}$$

$$R_{f2}^2 = R_{b2}^2 + [(R_{b2}-R_{bc})\tan\phi_2^c + \sqrt{(R_{hc}^2 - R_{bc}^2)}]^2 \quad \text{(A22)}$$

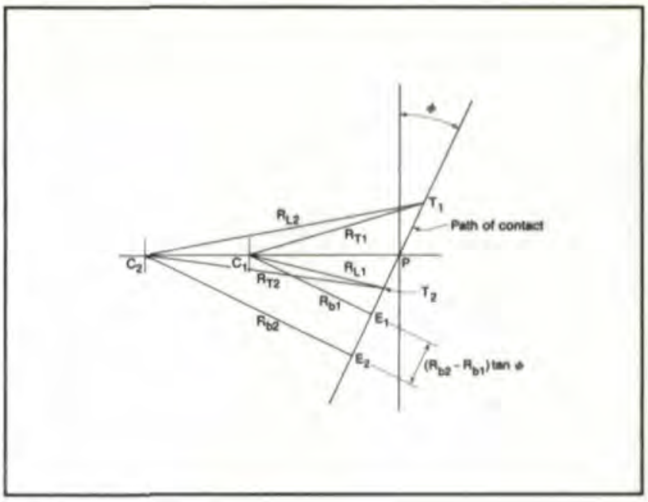

Fig. 10

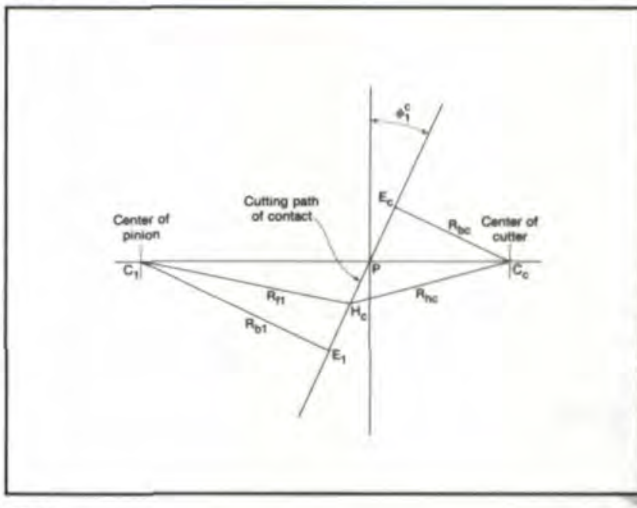

Fig. 11

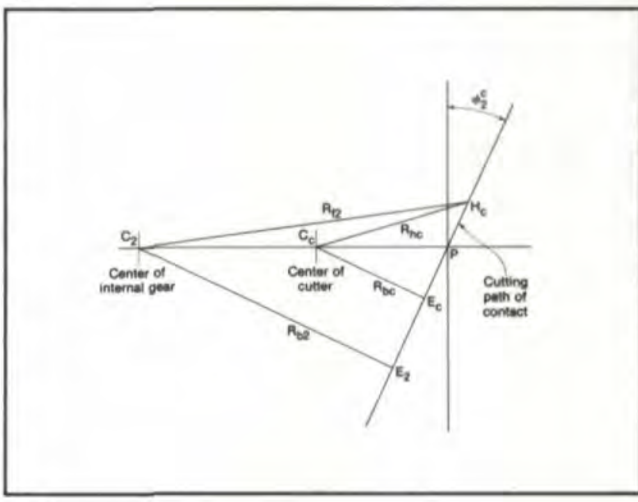

Fig. 12

References

1. J.R. COLBOURNE. *The Geometry of Involute Gears.* Springer Verlag, New York, May, 1987.
2. J.W. POLDER. "Interference and Other Limiting Conditions of Internal Gears," ASME Paper 84-DET-180, presented at the ASME Design and Production Engineering Technical Conference, Cambridge, Mass., October, 1984.

Acknowledgement: *Reprinted with premission of the American Gear Manufacturers Association. The opinions, statements, and conclusions presented in this paper are those of the Author and in no way represent the position or opinion of the AMERICAN GEAR MANUFACTURERS ASSOCIATION.*

Back To Basics

Shaper Cutters — Design & Application—Part 2

William L. Janninck
ITW — Illinois Tools, Lincolnwood, IL

Editor's Note: This is part two of a feature begun in our last issue. In the Mar/Apr issue, Mr. Janninck discussed the shaping method, spur and helical cutters, herringbone cutters, cutter blank sizes, tooth shape change, tooth forms, and cutting internal gears.

Cutter Sharpening

Cutter sharpening is very important both during manufacturing and subsequently in resharpening after dulling. Not only does this process affect cutter "over cutting edge" quality and the quality of the part cut, but it can also affect the manner in which chip flow takes place on the cutter face if the surface finish is too rough or rippled.

The sharpening of spur cutters and those helicals under 8° helix angle that are made with a conical sharpening, are usually sharpened on a rotary table surface grinder using a centering plug, and with the table set at the sharpening angle. See Fig. 2-1. The sharpening angle has been standardized at 5°, so normally the table is set at 5°. Small downfeeds are used along with a good coolant flow to prevent material burn. No wavy pattern should appear.

The cutter manufacturer would recommend using two separate grinding operations, one a roughing pass with a coarser grit, and the second with a fine grit to get a fine, almost polished finish on the tooth face. Usually for expediency only, one operation is used.

The sharpening of helical cutters with the step-sharpening, as seen in Fig. 2-2, which is also called normal sharpening, requires more elaborate equipment. A surface grinder fixture which contains the geometric requirements is shown in Fig. 2-3. These fixtures have been made in several styles and are usually used in small shops. The fixture is usually made with a 5° angle. Fig. 2-4 shows a view of the sharpening plane on the cutter tooth face and the face sharpening angle.

For quantity sharpening of stepped face cutters, say on a high production gear line, specially constructed machines with automatic operation are used.

While the standard practice is to place the cutting face normal to the cutter helix, experience has proven a benefit in cutter utility by considering the off-normal sharpening. This is called a chip control sharpening, and the helical sharpening angle is usually 8° less than the cutter helix angle. See Fig. 2-5.

Cutter Lead Guides

For a spur cutter the reciprocation takes place in a straight line; thus, for all spur cutters a single spur guide is used in moving the cutter along a straight path.

For a helical cutter a helical guide of the same hand and lead as the cutter being used must be available. As a helical cutter is reciprocated it must pass the cutter teeth through a helical lead path. See Fig. 2-6 for a schematic view of the functioning of typical spur and helical lead guides.

For a vertical axis machine, the guide and shoe are usually located on the top end of the cutter ram, where they are accessable for changing. Lead guides are a required setup item.

Frequently the gear manufacturer wants to utilize lead guides that are available in-house, avoiding extra cost and possible delay in procurement. First, confirmation is made of the hand of guide and cutter. Then a comparison is made of the lead of guide and gear and number of teeth of cutter and gear according to this formula:

$$\frac{\text{LEAD OF GEAR}}{\text{GEAR TEETH}} = \frac{\text{LEAD OF GUIDE}}{\text{CUTTER TEETH}}$$

If the data meets equality in this equation, the guide can be used. Varying the cutter teeth or altering the gear data may find a solution.

Gear Clearance Grooves

When cutting a gear located adjacent to a shoulder, it is necessary to provide a groove for the cutter to pass into at the bottom of the stroke. Fig. 2-7 shows such a case for a spur cutter. Depending on the helix angle and the type of sharpening used, the groove width for helical gears will usually be wider. See Fig. 2-8.

Indicating Diameters

An accurately ground ring located on the shoulder diameter just behind the teeth of a disk or deep counterbore

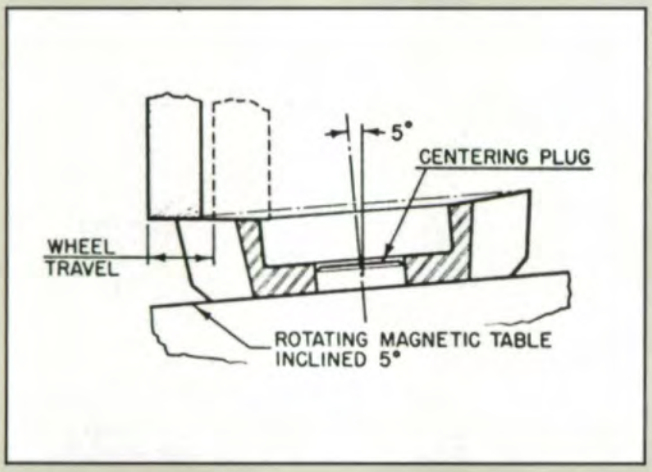

Fig. 2-1 – Circular sharpening of a cutter.

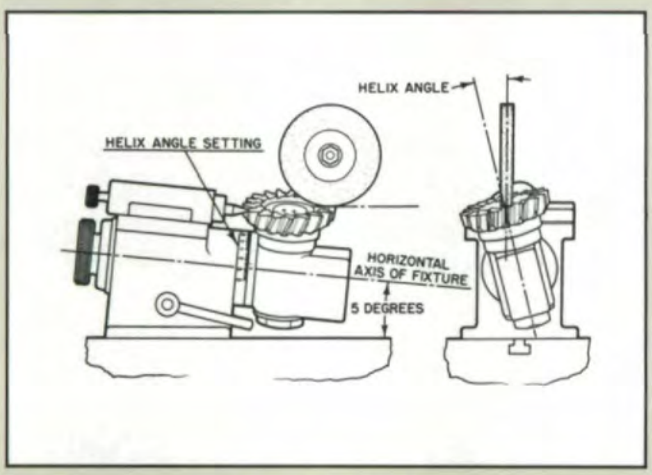

Fig. 2-2 – Helical cutter with step sharpening and its cut gear.

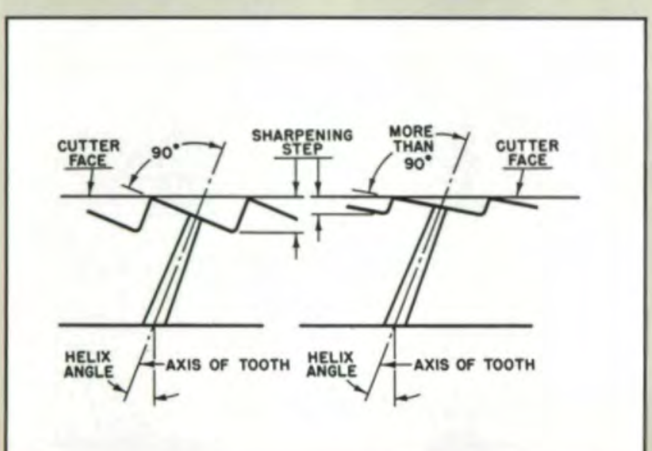

Fig. 2-3 – Helical cutter sharpening fixture.

Fig. 2-4 – Normal sharpening plane.

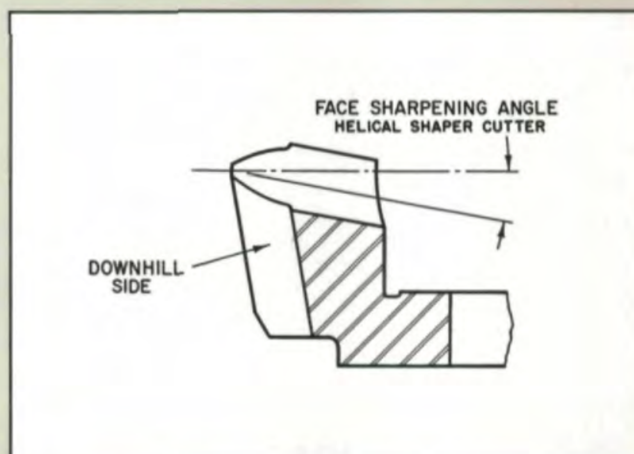

Fig. 2-5 – Normal and chip control sharpening.

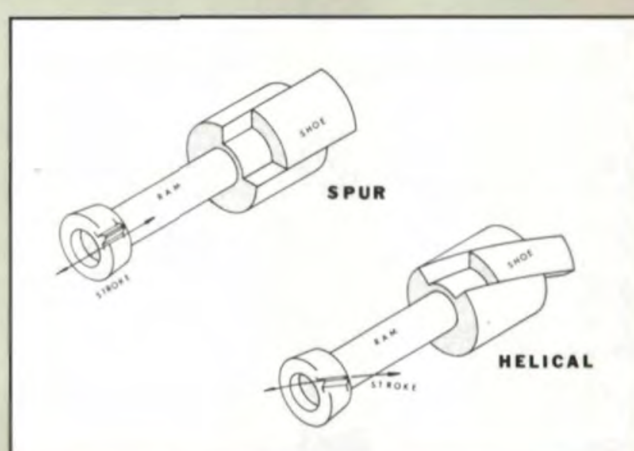

Fig. 2-6 – Diagramatic view of spur and helical lead guides.

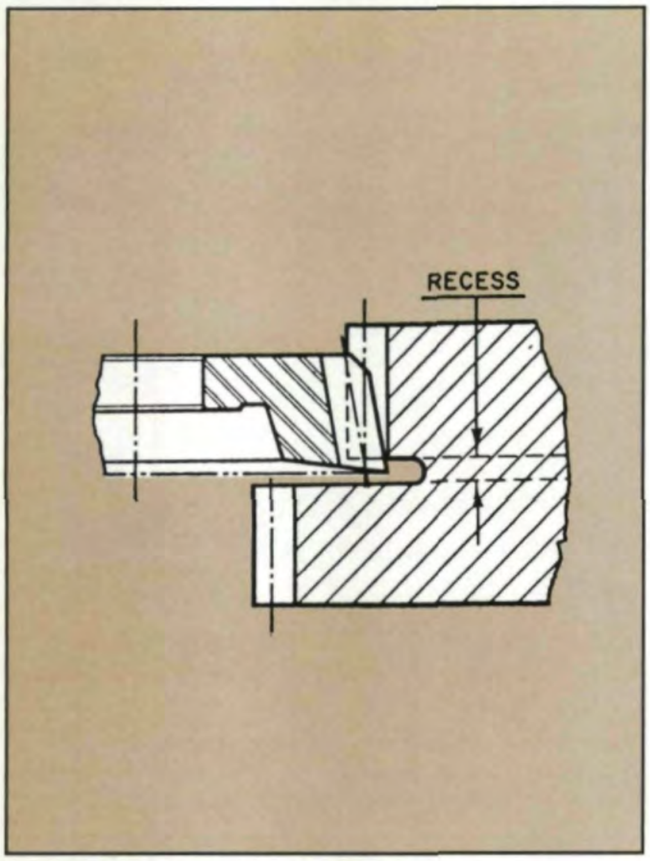

Fig. 2-7 – Clearance groove for a spur cutter.

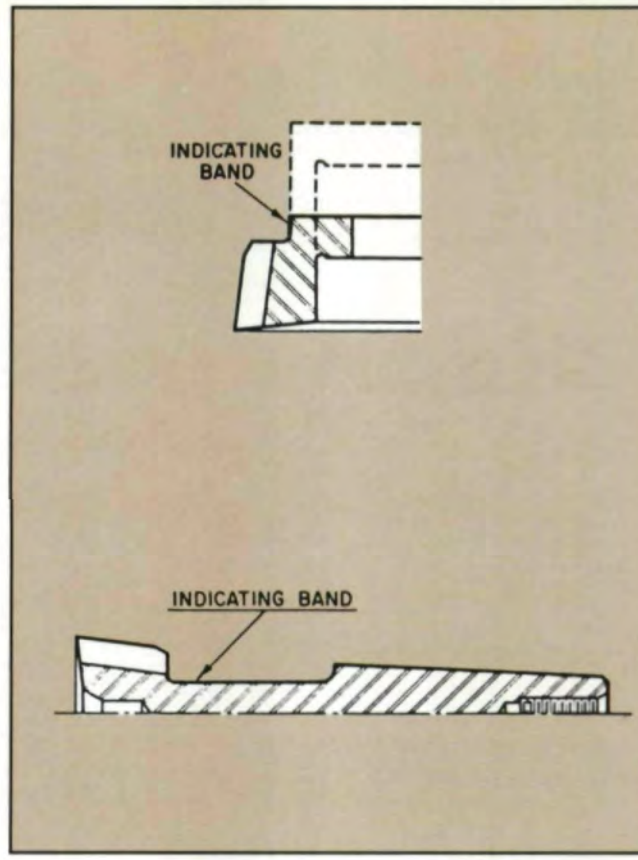

Fig. 2-9 – Cutter indicating rings.

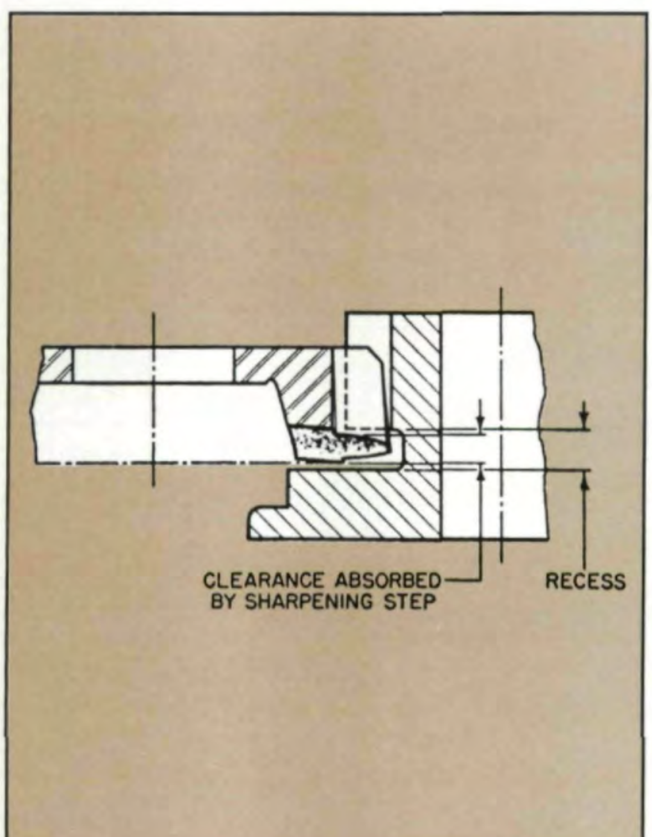

Fig. 2-8 – Clearance groove for a helical cutter.

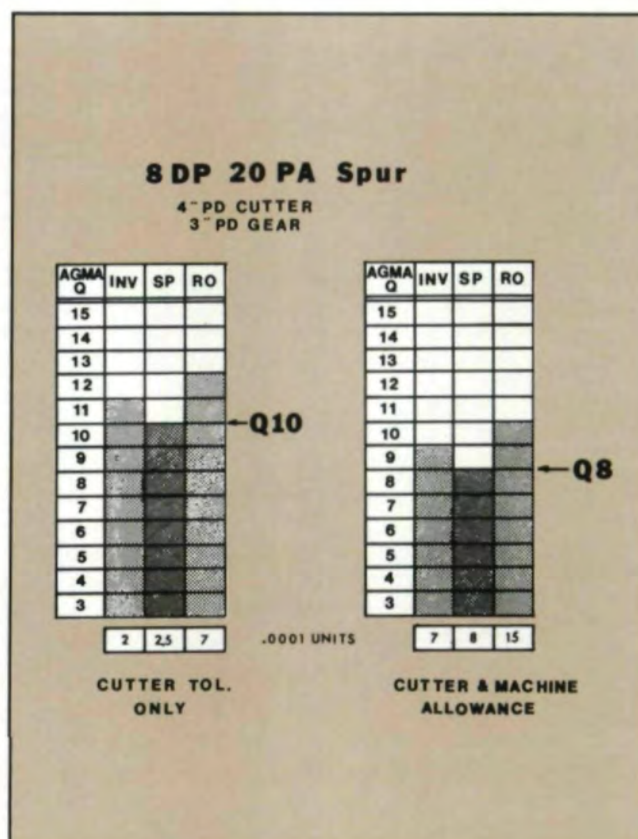

Fig. 2-10 – Shaper cutter accuracy capability.

shaper cutter, or on the diameter behind the teeth of a hub type or shank type cutter, is used as a truing ring for checking cutter runout while it is mounted in the gear shaping machine. See Fig. 2-9.

Cutter Tolerances

The first source for information on the tolerances for shaper cutters is the publication ANSI B94.21, "Gear Shaper Cutters." Only one level of accuracy is specified, which is called "Commercial Tolerance". MCTI, Metal Cutting Tool Institute, has similar standards which do include tolerances for "Commercial Ground" and, for certain cutter sizes only, tolerances for "Precision Ground".

Fig. 2-10 shows a comparison chart of what could be expected by cutting a gear using commercial tolerances, first, where only cutter tolerances are considered, and second, where some allowance is made for machine and machining influences. The best cutting ability is about AGMA Q-10 and, with allowances, about AGMA Q-8.

Tolerances are published for profile, spacing, and PD runout for the various types of cutter – disk, deep counterbore, shank, and herringbone. Tolerances are also given for bore, tooth thickness, flatness of cutter back, OD angle, sharpening angle, side relief angle, shank runout, shank diameter, indicating band runout, OD runout, and OD size. For herringbone cutters, matching tolerances on OD and width are given.

Cutter Base Circles

With the representation of the shaper

AUTHOR:

W.L. JANNINCK *is a consultant for ITW – Illinois Tools, a division of Illinois Tool Works, Inc. He has nearly 40 years' experience in an engineering and manufacturing environment in a cutting tool plant working in the design, development, and application of gear shaper cutters and gear hobs used in the generating process of gear cutting. He has served on various committees of AGMA and MCTI and is past chairman of the AGMA Cutting Tools Committee. He has also served on the SAE – ANSI Involute Spline Committee and ASME – Committee on Power Transmission Chains and Sprockets. He has written several articles on tool applications, gaging, gear design, and gear inspection.*

Fig. 2-11 – Single flank generating grinder.

cutter as a gear, it is also inspected on an involute checking instrument. The base circle diameters are not the theoretical ones expected, but are corrected for the cutting clearances on the cutter. For a spur cutter the base diameters are the same on both flanks, right and left. With the additional geometry of the helix and normal sharpening on a helical cutter, base circles differ from side to side.

The base diameters of spur or helical cutters are constant throughout the life of the cutter.

Because of the need to maintain a cutting edge in the transverse plane, herringbone cutters are not corrected, and the base diameter is equal to the theoretical value and is the same on both flanks.

Cutter Generation

The traditional process used in making shaper cutters is by abrasive wheel grinding, which can provide both a good finish and accuracy. All processes use some form of involute generation, whether it be a single flank grind using the radial side of the grinding wheel, such as seen in Fig. 2-11, or using a dual flank grind with a reciprocating vee-shaped wheel, as is shown in the diagram in Fig. 2-12. Another method using a ribbed or threaded abrasive wheel running in timed relation to the cutter has been used for some unmodified fine diametral pitch tools.

The single flank method requires a *large wheel relative to the cutter width* and is positioned tangent to the cutter tooth flank. The wheel position is stationary, and the cutter is rotated and translated below the wheel to generate the involute. Each flank is ground separately, and the number of teeth is established by an indexing mechanism.

The dual flank grinder uses a vee-shaped grinding wheel dressed to generate the form required on the cutter. The cutter is rolled tangent to a generating circle and passed or translated through the reciprocating grinding wheel. Indexing takes place at the end of a generation cycle. The entire profile of the cutter, tip, root, and both flanks can be ground at one time with one space being completed between indexing cycles.

Fig. 2-12 – Dual flank generating grinder.

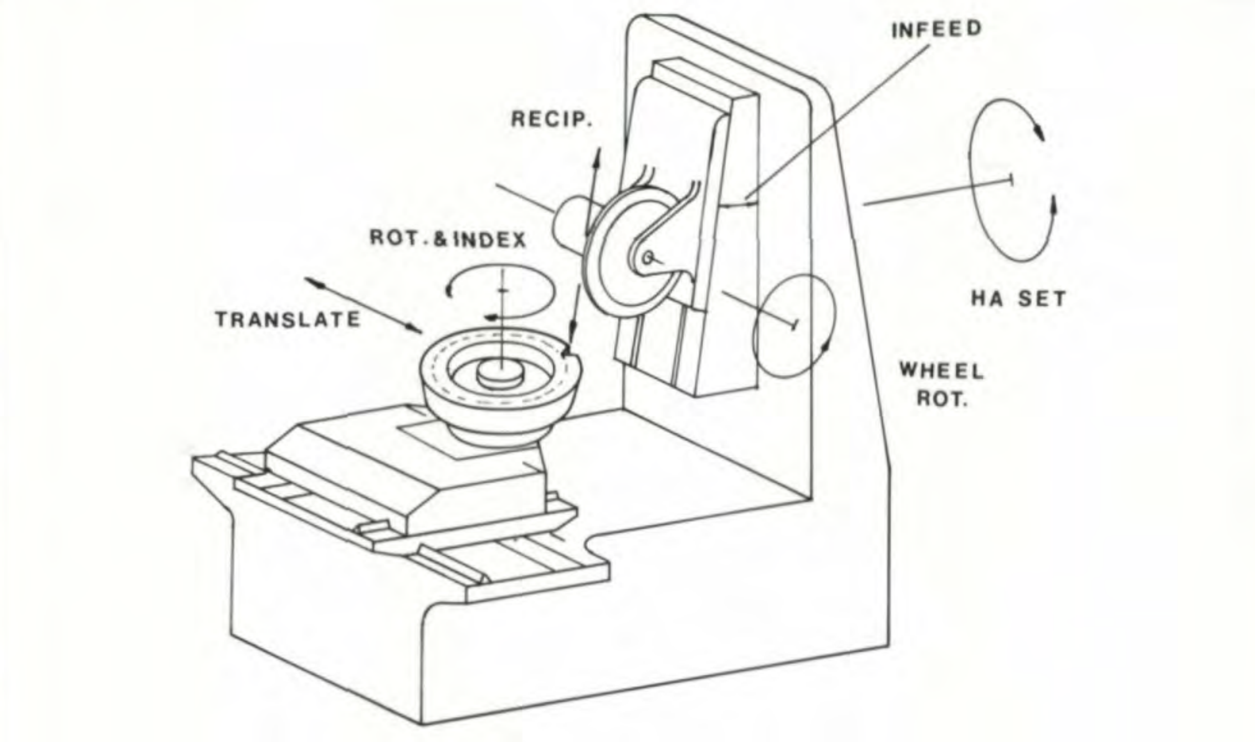

Fig. 2-13 – Machine mounting of various cutter types.

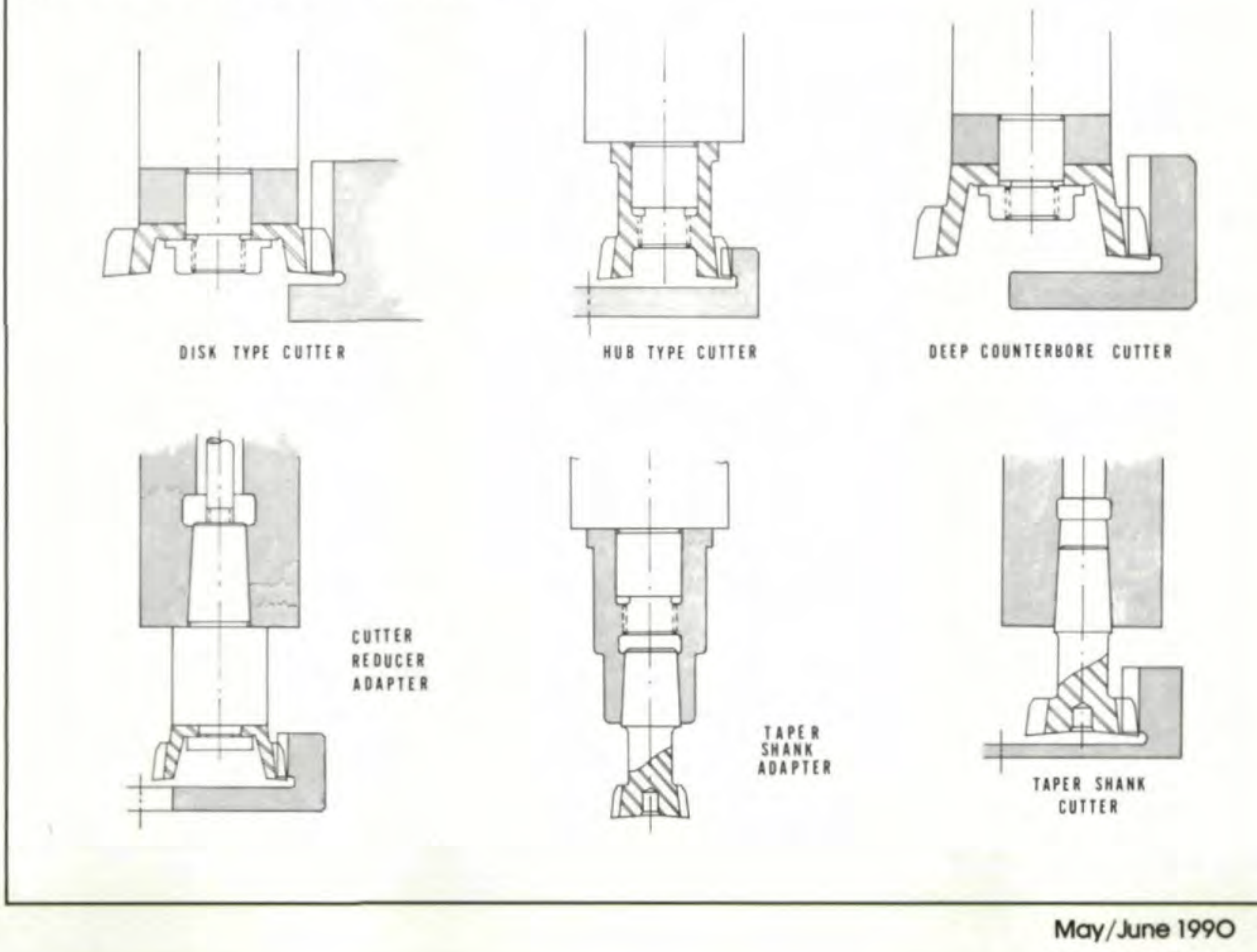

Cutter Clearance Angles

The side relief angle of a shaper cutter generally ranges between 1.5° and 2.5°, with the norm being 2.0°. This is a relatively low amount of clearance for a metal cutting tool, and any substantial increase in this angle can cause drastic changes in cutter geometry and design and would reduce useful cutter life.

The cutter outside angle is a function of cutter-gear geometry, amount of side relief, and pressure angle. It ranges approximately from 3.5° for 30PA to 5.5° for 20PA and 8.5° for 14.5PA. The geometrically true cutter outside angle is not usually a straight angle, but is really a curve that is compromised to a straight line. The cutter designer must be fully aware of the deviation amount in order to make proper allowances.

Cutter PD

The cutter PD is defined in the same way as an equivalent gear using the same formulae. With shaper cutters the PD is frequently referred to in a general way, such as a 3" or 4" PD cutter, meaning a nominal or approximate size.

Cutter Oversize and Undersize

In optimizing cutter life and utility it is normally expected that a cutter will be made somewhat oversize or larger on diameter than standard. Some gear geometries may require that a gear be made undersize or less than standard on diameter.

Design Optimization

In the process of designing a gear shaper cutter, several possible extremes are considered. Going toward a maximum oversize design will reduce cutter tip land toward a sharp. Setting a practical limit on the tip flat and maintaining proper part geometry will yield the maximum oversize cutter.

In consideration of the smallest possible diameter undersize for the cutter without damaging effects on the cutter or part, the targeted end life point on the cutter is determined. With allowance for other factors in the total tool layout, the final design will fall in between these limits. Such designs are usually computer aided and are planned solely for one part.

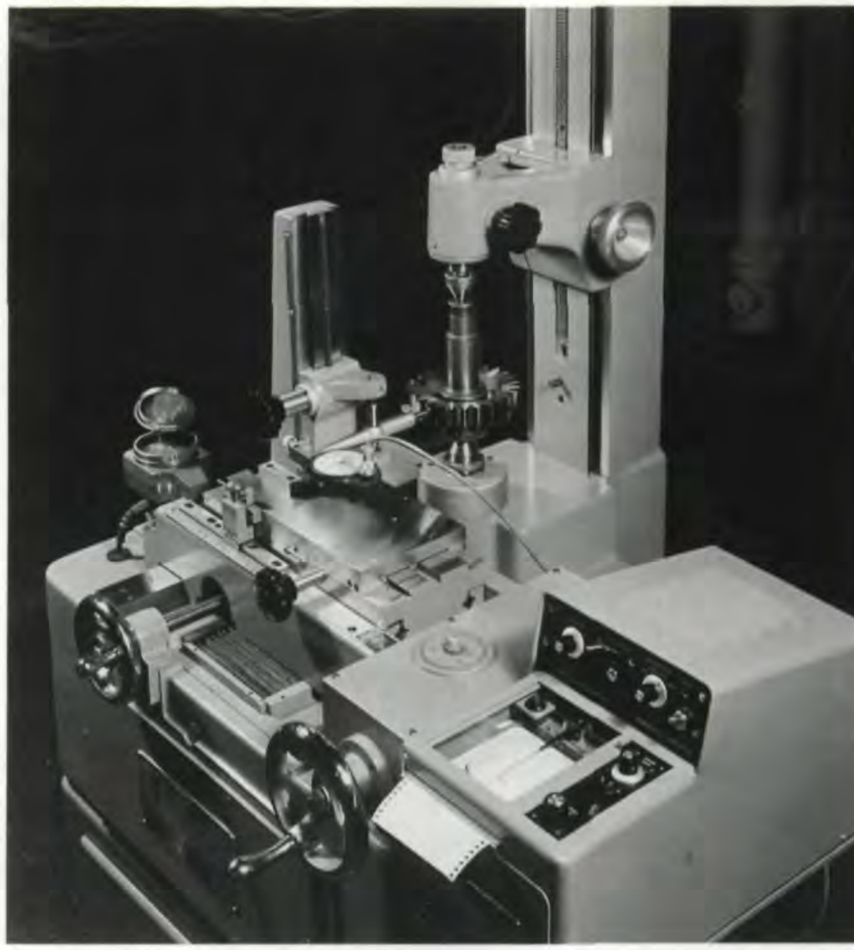

Fig. 2-14 – Involute profile inspection of a cutter.

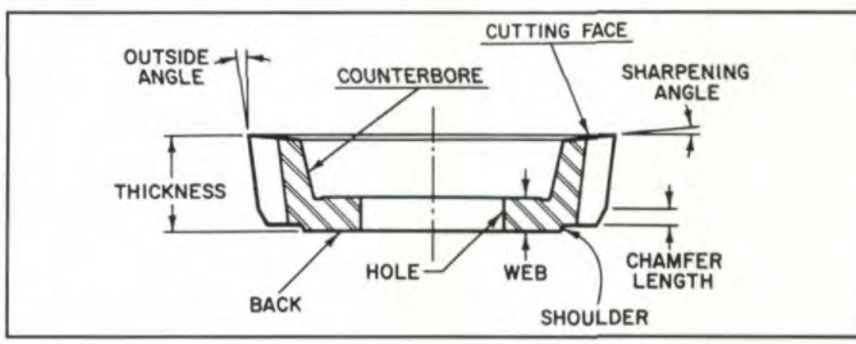

Fig. 2-15 – Cutter blank definitions.

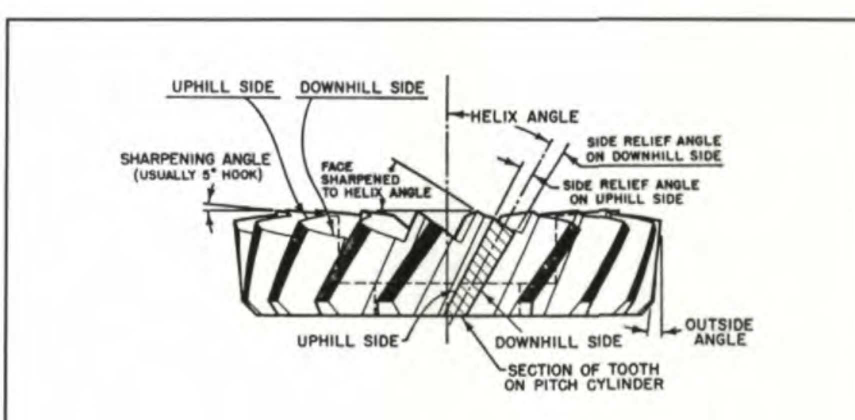

Fig. 2-16 – Helical cutter definitions.

Fig. 2-17 — Roller chain sprocket cutter.

Fig. 2-18 — Tandem cutter.

Fig. 2-19 — Cutter with teeth removed.

Fig. 2-20 — Groove and lip sharpening on herringbone cutter.

Keyways

Keyways are used on some shaper cutters, especially on helical cutters, where there is some chance that the cutter may slip rotationally under load. Herringbone cutters, always helical, use a keyway in the bore. Most other cutters use a slot in the mounting face. Another purpose of the keyway is for timing or alignment. Examples of keyways can be seen in some of the figures.

Cutter Mountings

Shaper cutters are made in various types to suit the special needs for application to the part or cutting machine. Fig. 2-13 illustrates various ways that these cutters can be mounted. While disk and deep counterbore cutters are fairly secure in their mountings, any long shank type cutter, including those used with taper or straight shank adapters, should be checked for possible excessive runout.

Cutter Inspection

Shaper cutters are inspected in a similar fashion to gears using some of the same involute, lead, and spacing instruments. Fig. 2-14 shows a view of a cutter during the involute profile check.

Nomenclature

Cutter nomenclature has been listed in several publications including the ANSI standard. Fig. 2-15 shows some of the terminology for a hole type cutter, and Fig. 2-16 illustrates some of the helical element definitions. Figs. 2-17 – 2-20 show cutters of various types and conditions.

Tool Materials

Most cutters are made of AISI M-2, M-3, and M-4 high-speed steels with some special applications of part material alloy content, part hardness, or material abrasiveness requiring the super materials, such as M-42, T-15, or Rex 76. Most of these materials are available in the particle metal process.

The titanium nitride coatings are also being used successfully on gear shaper cutters.

Acknowledgement: *Presented at the SME Gear Processing and Manufacturing Clinic, November 1-3, 1988. Reprinted with permission of the Society of Manufacturing Engineers.*

Classified

Service

GEAR TESTING AND DESIGN FACILITIES

- GEAR DESIGN (NOISE – STRENGTH).
- ROTATING GEAR (TORQUE – SPEED CONTROL) TEST MACHINES.
- SINGLE TOOTH BENDING FATIGUE TESTING.
- STATISTICAL PLANNING – ANALYSIS.
- WROUGHT STEELS, SINTERED METALS, NON-METALLIC MAT'LS.
- CAD FACILITIES FOR LOW COST SET-UP.
- CUSTOM TEST MACHINE DESIGN.
- EXPERIENCED PERSONNEL.

PACKER ENGINEERING
708/355-5722, ext. 214
BOX 353, NAPERVILLE, IL 60566

CIRCLE A-23 ON READER REPLY CARD

GEAR TOOTH GRINDING SERVICES

- Production and Prototype Quantities
- Specialists in Gear Tooth Grinding
- Able to match delivery to your needs
- Gear Tooth Grinding Capacity to 27.5 inch pitch diameters
- All services to AGMA standards

CERTIFIED GEAR INSPECTION

PRO-GEAR COMPANY, INC.
23 Dick Road
Depew, NY 14043
Phone (716) 684-3811
Fax (716) 684-7717

Sales Reps. Wanted

CIRCLE A-24 ON READER REPLY CARD

OPEN TIME

PRECISION GEAR INCORPORATED
CORONA, NEW YORK

Has Open Time!

- Pfauter PE 300
- Lorenz 424 Shaper
- Kapp VAS 432 Borazon
- Gear Grinding (External to 12")
- From AGMA 10

Fax Steve Gerard with your requirements
718-592-2525

CIRCLE A-25 ON READER REPLY CARD

Heat Treating Service

Contour Induction Hardening Specialists

Spur, helical and bevel gears

Our gear hardening equipment includes 4 NATCO submerged process machines and 3 AJAX CNC-controlled gear scanning machines. We can also tool to meet any production need. Write for a free brochure.

American Metal Treating Company
1043 East 62nd Street
Cleveland, OH 44103
(216)431-4492
Fax: (216)431-1508

CIRCLE A-26 ON READER REPLY CARD

SOPHISTICATED GEAR HARDENING

FULL SERVICE HEAT TREATERS SPECIALIZING IN

- Induction and Flame Hardening
  - Internal & External Natco Gear Hardening
  - Coil Induction Hardening
  - Gear, Shaft & Roll Flame Hardening
- Aerospace Spec Carburizing & Hardening
  - Gleason Press Quenching
  - Large 48x72x36 Integral Quench Furnaces
  - Hot Oil Quenching
  - Deep 126 in. Pit Furnace
- Subzero Treatment
- Aluminum
- Military Specifications
- Stainless
- Metallurgical Consulting

The Symbol of Quality & Service

The Cincinnati Steel Treating Co.
5701 Mariemont Avenue
Cincinnati, Ohio 45227
(513) 271-3173
Fax (513) 271-3510

CIRCLE A-27 ON READER REPLY CARD

Gear Tools

GEAR HOBS, CUTTERS GEAR MACHINES

Hundreds of New, Fully Ground Gear Hobs and Gear Shaper Cutters in stock at *LOWEST PRICES EVER!*

GEAR HOBS

2 TO 5 MODULE
3 TO 16 DIAMETRAL PITCH

GEAR SHAPER CUTTERS

4 TO 12 DP, 4" PITCH DIAMETER
8 TO 24 DP, 3" PITCH DIAMETER

WE CARRY A COMPLETE LINE OF NEW GEAR MACHINES: SHAPERS, HOBBERS, SHAVERS, HONERS, GRINDERS, SPLINE MILLERS, RACK SHAPERS, TESTERS etc.

CALL NOW FOR MORE DETAILS
(213) 933-0311

INTERCONTINENTAL INDUSTRIES INCORPORATED
P.O. BOX 36329, LOS ANGELES, CA 90036 FAX (213) 933-7487

CIRCLE A-28 ON READER REPLY CARD

Rates: Line Classified – per inch - $175
Classified Display – per inch (3" min.)
1X-$140, **3X**-$130, **6X**-$120. Type will be set to advertiser's layout or *Gear Technology* will set type at no extra charge.

Payment: Full payment must accompany classified ads. Send check or Visa/Mastercard number and expiration date to: *Gear Technology*, P.O. Box 1426, Elk Grove Village, IL 60007.
Agency Commission: No agency commission on classifieds.

Materials Deadline: Ads must be received by the 25th of the month, two months prior to publication. **Acceptance:** Publisher reserves the right to accept or reject classified advertisements at his discretion.

Gear Blanks

Literature

Computer Aids

Help Wanted

(continued from page 16)

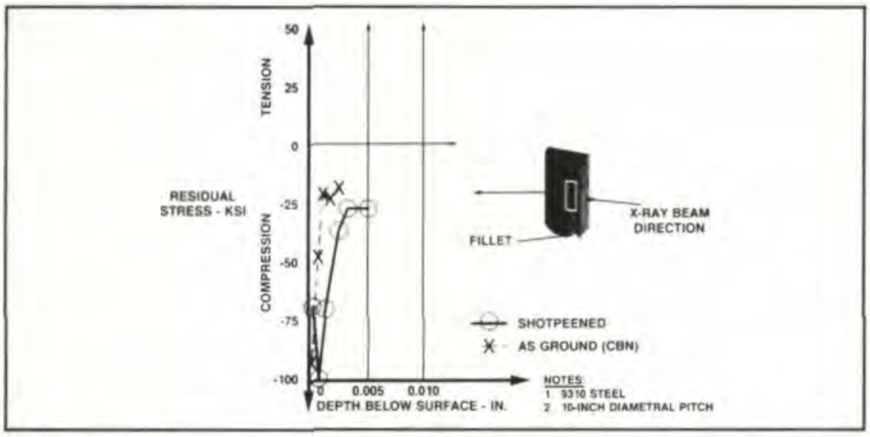

Fig. 19 – Residual stresses for CBN-ground gears.

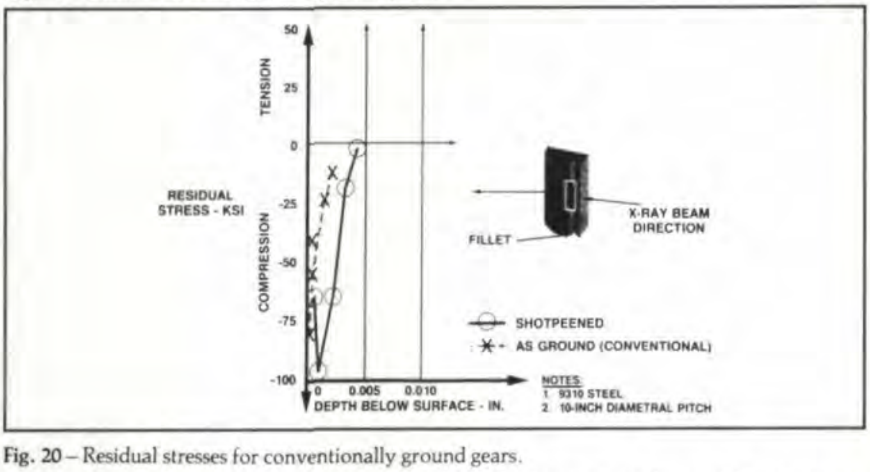

Fig. 20 – Residual stresses for conventionally ground gears.

Comment

While the data presented herein do not demonstrate any improvement in load capacity for CBN-ground gears, they do show this to be a viable process for finishing helicopter gears. The discrepancy in reported improvements in load capacity reported elsewhere in the literature may be more easily understood if a few points are kept in mind.

Many of the reports of improved load capacity are based on comparisons that are not truly "apples-to-apples". For example, Kimmet[4] cites such an improvement by noting that". . . CBN ground gears have a significantly longer fatigue life as compared with conventionally processed gears." However, the conventionally processed gears in that case were carburized and lapped, not carburized and conventionally ground; the latter would have made a more valid comparison. Other cases have been reported in which CBN gears have replaced conventionally ground gears with improved performance. This too, is probably a correct, but incomplete observation. The author can cite a very convincing example in his own experience in which a set of CBN-finished gears was used to replace a set of ground gears that were experiencing premature failure. The result was that the CBN gears did, in fact, solve the early failure problem. However, the truth of the matter was that the conventionally ground gears were abusively ground; this lack of proper grinding technique resulted in the failures observed.

It is far easier to produce properly finished CBN gears than conventionally ground gears. This is the main advantage in load capacity, not any inherent property of the processing itself. As demonstrated herein, properly processed conventionally ground gears do, in fact, have a statistically insignificant edge in terms of load capacity.

Conclusions

Based on the results of this program, we have reached the following conclusions specifically related to helicopter-quality AISI 9310 vacuum-melt gears finished by conventional and CBN grinding:

1. CBN-ground gears provide equivalent performance to conventionally ground gears of identical geometry and metallurgy.
2. CBN grinding, when compared to properly processed conventionally ground gears, provides no improvement in load capacity or fatigue life.

References:

1. General Electric Company Product Data Sheet SMD 18-410.
2. DEVRIES, R.C. *Cubic Boron Nitride: Handbook of Properties,* General Electric Company, Report No. 72CRD178, June, 1972.
3. CLUFF, B.W. "An Emerging Technology: Form Grinding With Borazon," paper presented at the American Gear Manufacturers Aerospace Gearing Committee Meeting, San Diego, CA, February, 1982.
4. KIMMET, G.W. "CBN Finish Grinding of Hardened Spiral Bevel and Hypoid Gears," AGMA Paper 84FTM6, American Gear Manufacturers Association Fall Technical Meeting, Washington, DC, October, 1984.
5. KUMAR, D.V. "Technological Fundamentals of CBN Bevel Gear Finish Grinding," SAE Paper MR85-273, Society of Automotive Engineers Conference on Superabrasives 1985, Chicago, IL April, 1985.
6. CHUKWUDEBE, L.O. "Grinding with Borazon CBN, Diamond/CBN Abrasives - A New Status for Super-abrasives," Symposium presented by the Diamond Wheel Manufracturer's Institute, November, 1975.
7. ALBRECHT, C., "Statistical Evaluation of a Limited Number of Fatigue Test Specimens Including a Factor of Safety Approach," Boeing Helicopter, TP102, Presented at the Fourth Pacific Area National Meeting of the American Society for Testing and Materials, Los Angeles, CA, 1962.

Acknowledgement: *Printed with permission of the copyright holder, the American Gear Manufacturer Association. The opinions, statements and conclusion presented in the paper are those of the Author and in no way represent the position or opinion of the AMERICAN GEAR MANUFACTURERS ASSOCIATION.*

TRUE CBN WHEELS

EFFICIENTLY AND EASILY, OFF MACHINE, WITH THE

NORMAC
CBN5 PROFILING CENTER

Made in U.S.A. (Patent No. 4,559,919)

The Normac **CBN5 Profiling Center** is ideal for off-machine trueing and re-forming of CBN grinding wheels, and form dressing conventional grinding wheels. The **CBN5** features the **FORMASTER** grinding wheel profiler with a general numeric 810M CNC, and a variable speed wheel spindle with capacity for up to 18" (457 mm) diameter grinding wheels up to 2" (50 mm) wide. The **FORMASTER** uses a variable speed rotary diamond dressing wheel, the trueing method recommended by CBN grinding wheel manufacturers. The **CBN5** can also be used for pre-forming production grinding wheels to save expensive production machine time.

NORMAC, INC.

NORMAC, INC.
P. O. Box 69
Arden, NC 28704
Phone: (704) 684-1002
Fax: (704) 684-1384

NORMAC, INC.
P.O. Box 207
Northville, MI 48167
Phone: (313) 349-2644
Fax: (313) 349-1440